Org Divers Evol (2011) 11:201–236
DOI 10.1007/s13127-011-0048-0

ORIGINAL ARTICLE

ORGANISMS DIVERSITY & EVOLUTION

Interactive 3D anatomy and affinities of the Hyalogyrinidae, basal Heterobranchia (Gastropoda) with a rhipidoglossate radula

Gerhard Haszprunar · Erika Speimann · Andreas Hawe · Martin Heß

Received: 25 January 2011 / Accepted: 26 May 2011 / Published online: 19 June 2011

Abstract Whereas *Hyalogyrina* Marshall, 1988 was originally considered a skeneid vetigastropod, the family Hyalogyrinidae Warén & Bouchet, 1993 has later been classified as basal Heterobranchia despite their rhipidoglossate radula. In order to evaluate this placement and to shed more light on the origin of all higher Gastropoda, we investigated five representatives of all three nominal hyalogyrinid genera by means of semithin serial sectioning and computer-aided 3D reconstruction of the respective anatomy, which we present in an interactive way. In general the morphological features (shell, external morphology, anatomy) fully confirm the placement of Hyalogyrinidae in the Heterobranchia, but in particular the conditions of the genital system vary substantially within the family. The ectobranch gill of Hyalogyrinidae is shared with Valvatidae, Cornirostridae, and Xylodisculidae; consequently all these families are united in Ectobranchia Fischer, 1884. The rhipidoglossate hyalogyrinid radula suggests independent acquisition of taenioglossate radulae in the Caenogastropoda and other Ectobranchia. Therefore, the origin of the Heterobranchia—and thus of all higher gastropods—looks to have taken place already on the rhipidoglossate, i.e. the 'archaeogastropod', level of evolution. Ectobranchia are considered the first extant offshoot of the Heterobranchia; implications for the stem species of the latter are outlined.

Keywords Gastropoda · Ectobranchia · Hyalogyrinidae · Interactive 3D anatomy · Systematics · Phylogeny · Heterobranchia

Introduction

During the last 25 years major progress has been made in our understanding of the origin of the higher gastropods, i.e. the allogastropod, opisthobranch and pulmonate taxa, the latter two of which are commonly united as Euthyneura. Haszprunar (1985a) first proposed the "Heterobranchia-Concept" in considering certain former 'mesogastropods' as linking step by step a basal caenogastropod with a primitive euthyneuran level of organization. These (paraphyletic) 'allogastropods' (called heterostrophs by some authors) include, among other taxa, Ectobranchia = Valvatoidea, Architectonicidae and Mathildidae, Omalogyridae, and Rissoellidae; together with the euthyneuran groups these are classified as Heterobranchia. This concept of monophyly of all higher Gastropoda has been elaborated further by Salvini-Plawen and Haszprunar (1987) and Haszprunar (1988), and later confirmed by numerical cladistics of morphological characters (Ponder and Lindberg 1997) as well as by all applicable molecular analyses (Aktipis et al. 2008; Colgan et al. 2003; Dayrat and Tillier 2003; Dinapoli and Klussmann-Kolb 2010; Grande et al. 2008; Jörger et al. 2010; McArthur and Harasewych 2003; Wägele et al. 2008).

Based on detailed anatomical and ontogenetic studies by Rath (1986, 1988), Salvini-Plawen and Haszprunar (1987)

Electronic supplementary material The online version of this article (doi:10.1007/s13127-011-0048-0) contains supplementary material, which is available to authorized users.

G. Haszprunar (✉)
Zoologische Staatssammlung München,
Münchhausenstraße 21,
81247 Munich, Germany
e-mail: haszi@zsm.mwn.de

G. Haszprunar · E. Speimann · A. Hawe · M. Heß
Department Biology I and GeoBio-Center,
Ludwig-Maximilians-Universität München,
Großhaderner Str. 2,
82152 Planegg-Martinsried, Germany

and Haszprunar (1988) regarded the freshwater Valvatidae as the earliest, 'ectobranch' offshoot of the Heterobranchia. This assumption has been supported strongly by the discovery and detailed conchological (heterostrophic apex, though often masked by lecithotrophic mode of development), morphological, and spermatological (spiral type) examinations of marine valvatid relatives, namely the Cornirostridae, Xylodisculidae, and Orbitestellidae by Ponder (1990a, b), Healy (1990, 1993), and Warén (1992). In addition, Bandel (1991) described the Jurassic–Cretaceous fresh- to brackish-water family Provalvatidae as an extinct stem group of the Valvatoidea. The Devonian *Palaeocarbonaria jankei*, with heterostrophic shell apex and valvatoid shell shape, might be another relative (Bandel and Heidelberger 2002). Also recent molecular data suggest Ectobranchia Fischer, 1884 (in Fischer 1880–1887) as one of the earliest extant offshoots of Heterobranchia (Dinapoli and Klussmann-Kolb 2010; Jörger et al. 2010).

The features of the heterobranch stem species and the most likely sister group of Heterobranchia are still matters of debate: Whereas Haszprunar (1988) considered a common, monophyletic origin of Heterobranchia and Caenogastropoda, Ponder (1991a) and Warén et al. (1993) provided counter arguments in favor of an independent 'archaeogastropod' (i.e. rhipidoglossate) origin of the Heterobranchia. Based on their numerical cladistic analyses, Ponder and Lindberg (1997) again preferred a monophyletic origin of Heterobranchia and Caenogastropoda, and proposed a taxon Apogastropoda for the combined clade. So far, the molecular data have significantly supported monophyletic Apogastropoda (e.g. Aktipis et al. 2008; Dinapoli and Klussmann-Kolb 2010).

More than 20 years ago, Marshall (1988) described several new gastropod genera and species from biogenic substrates at bathyal depths off New Zealand and New South Wales. According to their trochoid-like appearance and their rhipidoglossate radula, all of these species were originally classified among the Skeneidae, a lumping pot for small, trochoid-like forms. Two of Marshall's species, *Hyalogyrina glabra* and *Hyalogyra expansa*, were exceptional: While the protoconch is similar to those of other vetigastropods, there is more than one whorl, a condition unknown among the Trochoidea or Vetigastropoda in general (e.g. Bandel 1982). Nevertheless, also *Hyalogyra necrophaga* from the West African coast (Angola) was described by Rubio et al. (1992: fig. 3) as a skeneid vetigastropod despite a clearly visible hyperstrophic protoconch.

Warén and Bouchet (1993) described *Hyalogyrina grasslei* and *Hyalogyra vitrinelloides* from the hydrothermal vent habitats of the Guaymas and Lau basins, respectively, and provided SEM photographs of the shells, protoconchs, opercula, radulae, and heads. The authors erected the family Hyalogyrinidae for these and the two species by Marshall (1988) mentioned above, and proposed first the formal inclusion of the family within the Heterobranchia. In the same year Warén et al. (1993) reported on the shell, radula, and live animals of the Mediterranean *Xenoskenea pellucida* (first described by Monterosato 1874). The heterobranch nature of Hyalogyrinidae was strongly supported by spermatological data provided by Healy (1993) on *X. pellucida* and an unnamed "*Hyalogyrina*" species (possibly *Xylodiscula major* Warén & Bouchet, 1993) from hydrothermal vents off Fiji. A few years later Hasegawa (1997) described *Hyalogyrina depressa* from Japanese waters, and Warén et al. (1997) named *Hyalogyrina amphorae* and *Hyalogyra zibrowii* from the Mediterranean Sea. Later on, *Hyalogyrina umbellifera* and *H. globularis* were described again from hydrothermal vents by Warén and Bouchet (2001). Sahling et al. (2002) reported another, still unnamed *Hyalogyrina* species living at gas hydrate deposits from the Cascadia convergent margin in the North-East Pacific. Most recently Warén and Bouchet (2009) described *Hyalogyrina rissoella* from deep-sea hydrocarbon seeps off West Africa.

Thus, the Hyalogyrinidae presently comprise 13 extant species classified in three genera. *Alexogyra marshalli* Bandel, 1996 from the Early Triassic St. Cassian Formation might be added (Bandel 1996). However, the hyalogyrinid anatomy has remained virtually unknown, except for the data in a short summary (Speimann et al. 2007). Several preserved soft bodies of five hyalogyrinid species, which represent all three nominal genera (see below), were sent to the first author (GH) for detailed anatomical studies (see Acknowledgments). In order to provide a sound and thorough data basis for further considerations and hypotheses, we present here the detailed anatomical description of these species. Since all of them show helicoid shell and soft-part morphology and quite complicated conditions, particularly of their genital systems, the application of computer-aided 3D reconstruction and interactive 3D presentation is of particular advantage.

Material and methods

Material

Xenoskenea pellucida (Monterosato, 1874): The specimens investigated were collected in June 1988 during the "mission Algarve" by Serge F. Gofas in the East Atlantic off Portugal, Algarve (Chenal d'Olhao, 3–7 m, 37° 00′ N, 07° 51′ W), from muddy beds of *Zostera*. The sample has been preserved very well, but the semithin sections have been largely bleached by the sealing medium used about 20 years ago, cedar oil (see below).

Hyalogyrina glabra Marshall, 1988 is the type species of its genus, which itself typifies the family. Material from two

samples has been investigated: (1) Paratypes (BS 925, M. 74981: 42° 43.9′ S, 176° 08′ E to 42° 44.0′ S, 176° 05′ E, Chatham Rise, NE of Mernoo Bank, 800–810 m, 28 Sept. 1982, USSR f.v.Kaltan, stn. KTN/152/82) were found in/on a log of *Sophora microphylla* Ait. One classic section series (at 5 μm) and three semithin series (at 1 μm; blocks Y54, Y55, P93) have been made. (2) Further paratypes (M. 84295) from off Jackson Bay (43° 29.8′ S, 168° 54.1′ E, 900–945 m, coll. 15/2/1986) again lived on wood. Three further semithin section series (blocks 81A–83A) were made. Both samples were poorly preserved due to the original freezing (cf. Marshall 1988); again the sealing with cedar oil has unfortunately caused substantial bleaching.

Hyalogyrina depressa Hasegawa, 1997: Two paratypes from the type locality, Western Pacific off Japan (Suruga Bay, 35° 00.4′ N, 138° 43.9′ E to 35° 00.3′ N, 138° 42.6′ E, 400–740 m), were embedded and sectioned only 3 years ago.

Hyalogyrina grasslei Warén & Bouchet, 1993: Three paratypes from the type locality have been studied: Guyamas Basin, Alvin Dive 1613, about 2,000 m, "from retrieval box with *Riftia*." The original preservation was excellent, but the stained sections (made in 1991) have faded due to the sealing medium, so that phase contrast microscopy had to be employed to examine histological details.

Hyalogyra expansa Marshall, 1988: Two (BS 924, M.75002) plus one (M.87041) paratypes from the type locality (37° 23.87′ S, 177° 39.5′ E, off White I., New Zealand, alive on wood, 1,075–1,100 m, 23.xi.198 l, FV Kalinovo stn K01/19/81) were investigated. All specimens were poorly preserved due to the original freezing (cf. Marshall 1988), but the staining has remained unchanged.

All section series are deposited at the Zoologische Staatssammlung München (ZSM), Mollusca section (see Table 1).

Methods

Generally, specimens were originally preserved in seawater-buffered formalin (*Xenoskenea pellucida, Hyalogyrina grasslei*) or directly in 70% ethanol. All specimens were post-fixed with Bouin's fluid (concentrated formalin, picric acid, and concentrated acetic acid in the proportions 15 : 5 : 1), also to dissolve the shell. The remaining periostracum was recovered manually as far as possible. The specimens were rinsed several times with 70–80% ethanol with a drop of concentrated ammoniac solution until the fluid remained colourless (not yellowish).

After dehydration, one specimen of *Hyalogyra expansa* was embedded in paraffin (at 60°C), and serially sectioned (at 5 μm) with a regular microtome; the sections were deparaffinized with xylole and then stained by Heidenhain's Azan method (cf. Romeis 1989: p. 501).

All other specimens were embedded either in Spurr's (1969) resin or in Durcopan; after polymerization they were photographed in the resin block: In the latter the animal is very close to the bottom; therefore the blocks were orientated upside down, a drop of microscope oil was placed on the surface, and a cover glass added. In this arrangement in particular Nomarski Differential Interference Contrast (DIC) was very helpful for inferring the arrangement of various organ systems, especially the alimentary tract with jaws, radula, stomach, and rectum. The photographs were also used to improve the alignment of the section photos. Complete semi-thin section series (at 1–2 μm) were cut with Ralph knives according to Ruthensteiner's (2008) method, stained with methylene blue (Richardson et al. 1960), sealed with cedar oil and stored until recently. However, as outlined elsewhere (Hartmann et al. 2011) we now prefer and recommend direct sealing with the original resin to avoid bleaching.

Each semi-thin section of a selected series (Table 1) was digitally photographed on a regular optical microscope under bright-field illumination or—in cases of bleaching—in phase contrast. Computer-aided 3D reconstructions using the AMIRA software were done as described by Heß et al. (2008) and Hartmann et al. (2011). We followed the protocol by Ruthensteiner and Heß (2008) to create interactive 3D images for the PDF version of this publication (see the online edition of this ODE issue). In addition, high-resolution micrographs were made using bright-field or phase-contrast microscopy to show certain histological details.

The five species investigated differ significantly in their morphological details. Consequently, we provide separate descriptions of the respective anatomy and histology in the following results section, then compare features in the discussion section.

Results

Xenoskenea pellucida (Monterosato, 1874)

(Figures 1, 2, 3, 4, 5 and 6)

External morphology and foot

The epithelia of the head region are covered by a microvillous border, occasionally interspersed with ciliary tufts.

The foot is folded like a pocket knife in the preserved specimens, so that the operculum can close the shell aperture (Fig. 2a,b). There are no epipodial tentacles, but in most species one can see a ridge or lobe below the operculum. There are two pedal glands. The anterior one (Fig. 3b: ppg) opens via a wide pore at the anterior border

Table 1 Details and voucher deposition numbers of the section series of specimens investigated

Species	Sample	Embedding (block number)	Slide numbers, thickness	Preservation	Staining	ZSM inventory number
Xenoskenea pellucida	mission Algarve	Spurr (72A)	A1–A7, 2 μm	very good	Richardson, bleached	Mol 20110000
Xenoskenea pellucida	mission Algarve	Spurr (73A)	B1–B8, 2 μm	very good	Richardson, bleached	Mol 20110001
Xenoskenea pellucida	mission Algarve	Spurr (74A)	C1–C11, 2 μm	very good	Richardson, bleached	Mol 20110002
Xenoskenea pellucida	mission Algarve	Spurr (75A)	D1–D10, 2 μm	very good	Richardson, bleached	Mol 20110003
Hyalogyrina glabra	NMNZ, M.74981	Paraplast	A1–A3, 5 μm	poor, frozen	Azan, good	Mol 20110004
Hyalogyrina glabra	NMNZ, M.74981	Spurr (Y54)	B1–B13, 2 μm	poor, frozen	Richardson, bleached	Mol 20110005
Hyalogyrina glabra	NMNZ, M.74981	Spurr (P93)	C1–C8, 2 μm	poor, frozen	Richardson, bleached	Mol 20110006
Hyalogyrina glabra	NMNZ, M.74981	Spurr (Y55)	D1–D8, 2 μm	poor, frozen	Richardson, bleached	Mol 20110007
Hyalogyrina glabra	NMNZ, M.84295	Spurr (81A)	E1–E14, 2 μm	poor, frozen	Richardson, bleached	Mol 20110008
Hyalogyrina glabra	NMNZ, M.84295	Spurr (83A)	F1–F9, 2 μm	poor, frozen	Richardson, bleached	Mol 20110009
Hyalogyrina glabra	NMNZ, M.84295	Spurr (82A)	G1–G8, 2 μm	poor, frozen	Richardson, bleached	Mol 20110010
Hyalogyrina depressa	NSMT-Mo 70864	Epon (−)	A1–A14, 2 μm	good	Richardson, good	Mol 20110011
Hyalogyrina depressa	NSMT-Mo 70864	Epon (−)	B1–B9, 2 μm	good	Richardson, good	Mol 20110012
Hyalogyrina grasslei	Alvin 1613	Spurr (Y51)	A1–A22, 2 μm	very good	Richardson, bleached	Mol 20110013
Hyalogyrina grasslei	Alvin 1613	Spurr (Y52)	B1–B19, 2 μm	very good	Richardson, bleached	Mol 20110014
Hyalogyrina grasslei	Alvin 1613	Spurr (Y53)	C1–C10, 2 μm	very good	Richardson, bleached	Mol 20110015
Hyalogyra expansa	NMNZ, M.75002	Paraplast	A1–A5, 5 μm	poor, frozen	Azan, good	Mol 20110016
Hyalogyra expansa	NMNZ, M.75002	Durcopan (P91)	B1–B29, 2 μm	poor, frozen	Richardson, good	Mol 20110017
Hyalogyra expansa	NMNZ, M.87041	Spurr (79A)	C1–C13, 2 μm	poor, frozen	Richardson, bleached	Mol 20110018

NMNZ National Museum of New Zealand (Wellington); *NSMT* National Museum of Nature and Science (Tsukuba City, Japan); *ZSM* Zoologische Staatssammlung München (Bavarian state collection of zoology, Munich)

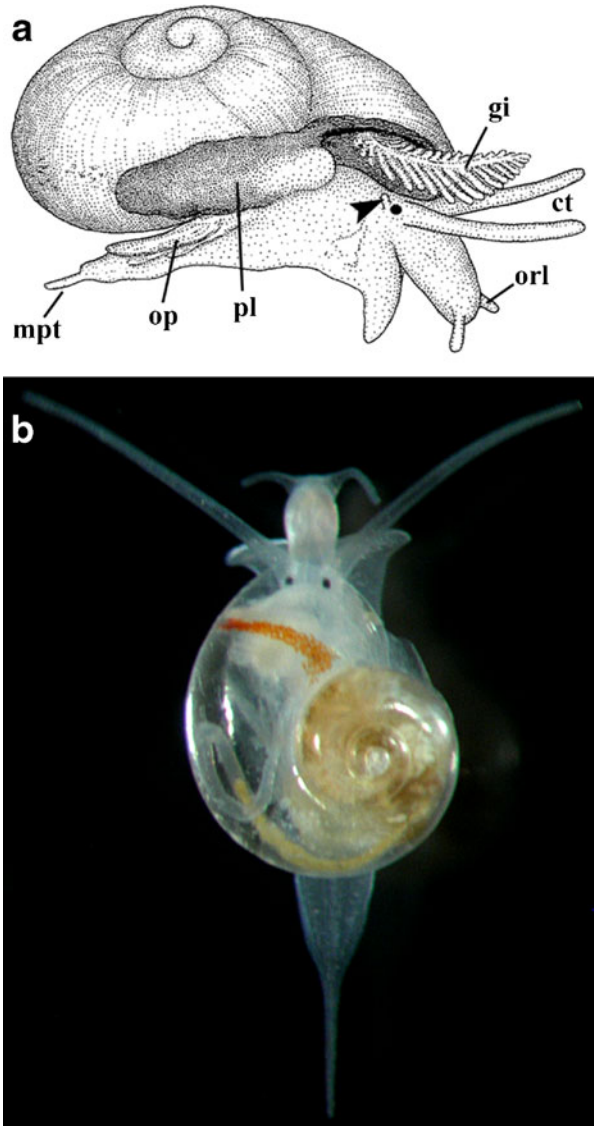

Fig. 1 *Xenoskenea* species. (**a**) *X. pellucida*, drawing of live animal (shell diameter 1.7 mm) from the right side (modified from Warén et al. 1993: fig. 35); arrowhead points to copulatory organ; labels: ct = cephalic tentacles, gi = gill (extended out of mantle cavity), mpt = metapodial tentacle, op = operculum, orl = oral lappet (in fact more a short tentacle), pl = pallial lobe. (**b**) *X.* n. sp. to be described by Dr. Kazunori Hasegawa; specimen data (courtesy of Dr. Takuma Haga, National Museum of Nature and Science, Tokyo): around Sandan-bashi (Sandan Bridge), Wakaura-Naka, Wakayama City, Wakayama Prefecture (central Honshû: W part of Kii Peninsula), Japan, 34°41′14″N, 135°10′25″E, 8 Oct. 2007, from aggregation of reen algae on muddy tidal flat, lower intertidal zone, leg. Haga, T., Fukuda, H., Yamashita, H., Tatara, Y. & Ikebe, S.; photo courtesy of Dr. Masanori Taru, Toho University, Funabashi, Japan

of the foot. The pore is continued backwards by a short (30 μm), broad and densely ciliated duct, which transports the mucus. This pedal gland is composed of very large (diameter 60–80 μm), round, heavily stained mucous cells. The posterior gland is composed of the same cell type, but the respective cells are smaller (diameter 40–50 μm). The gland duct opens at the center of the pedal sole, or in the fold in the contracted specimens. In addition, certain mucous cells of the same type and size release their content directly via narrow channels through the epithelium of the foot sole. These mucous cells are more common anteriorly, but are also found at the posterior foot sole.

The epithelium of the foot sole consists of highly cylindrical cells (25 μm×5 μm) and is densely ciliated throughout (Fig. 3b), whereas that of the back of the foot lacks cilia. Epithelial mucous cells with poorly stained content are very rarely interspersed.

The posterior foot tentacle (Figs. 1, 3d: mpt) is provided with a distinct retractor muscle but lacks all further specializations. The foot mass itself includes large haemocoelic spaces; muscle and collagen fibers are interspersed; parenchymous cells are rare. In the central part of the foot the connective tissue shows a dense aggregation of large, round, transparent calcium cells (Fig. 3e,f). These resemble mucous cells, but lack any connection to the exterior.

Mantle

The inner wall of the anterior mantle margin is mainly formed by small, cylindrical cells (with oval and compact nuclei). Ciliary tufts as well as mucous cells are interspersed. The anterior mantle margin is further characterized by very distinct, single globular cells. These cells (Fig. 3a) have a large vacuole in central position that contains an amorphous mucoid mass, which is released into the environment via a very narrow pore. The cytoplasm forms a hollow sphere around the vacuole, the nucleus is largely depressed. In addition, a complicated muscular grid of longitudinal and transversal muscles enables movement of the mantle.

At the anterior right corner the mantle forms a large pad. In all specimens the pad includes a thick, hollow tube with T-like lumen; in the sexually fully mature specimen the hollow tube was of much larger size and bulged back into the mantle cavity to the line of the rectal loop (see below). In retracted condition the opening of the tube lies close beneath the small copulatory organ with the opening of the vas deferens (see below). The epithelium of the tube is quite uniformly composed of cuboidal, sparsely ciliated cells with oval nuclei. Near the opening these cells are small (diameter 15–20 μm) and darker, more proximally they become continuously larger (diameter 25–30 μm) and less densely stained (Fig. 3c). The whole tube is surrounded by a grid of collagenous fibers of mainly longitudinal orientation and with longitudinally and transversally orientated muscle fibers. The anterior outer epithelium of the pad is identical to that of the anterior mantle margin, whereas the posterior part has the same histology as the mantle cavity (see below).

The inner wall of the posterior mantle margin is provided with a continuous sheath of heavily staining mucous cells, which open to the external environment.

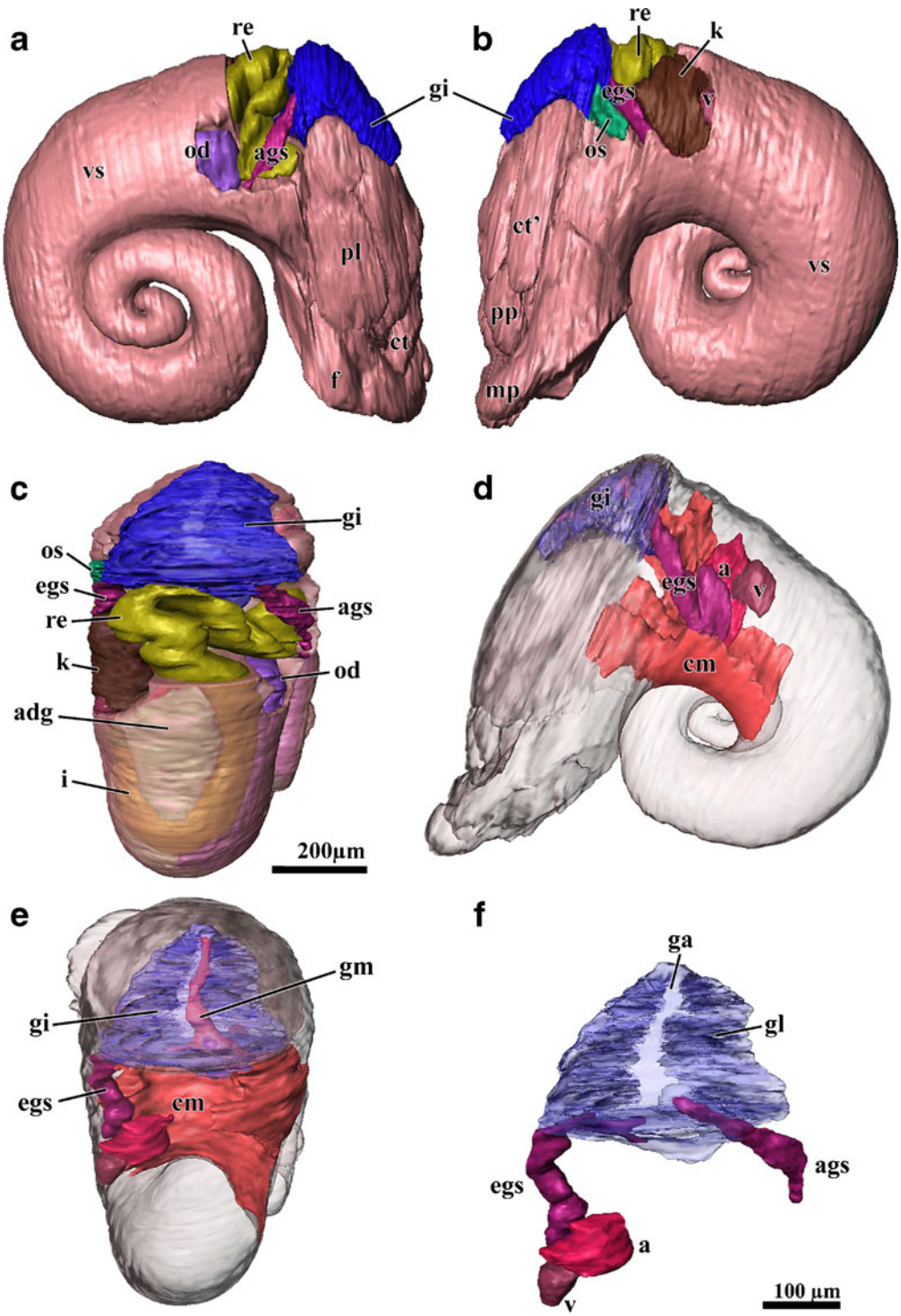

Fig. 2 *Xenoskenea pellucida.* **a**–**c** Reconstruction of mantle cavity and its organs; (**a**) right side view, (**b**) left side view, (**c**) dorsal view. **d**–**f** Circulatory and musclular system; (**d**) left side view, (**e**) dorsal view, (**f**) dorsal view of gill and associated blood sinuses. Labels: a = heart auricle, adg = anterior digestive gland, ags = anterior gill sinus, cm = columellar muscle, ct/ct' = right/left cephalic tentacle, egs = efferent gill sinus, f = foot, ga = gill axis, gi = gill, gl = gill lamellae, gm = gill muscle (retractor), i = intestine, k = kidney, mp = metapodium, od = oviduct, os = osphradium, pl = pallial lobe, pp = propodium, re = rectum, v = heart ventricle, vs = visceral sac. Supplementary plate 1 offers an interactive 3D model of *Xenoskenea pellucida* that can be accessed by clicking into Fig. 2 (Adobe Reader version 7 or higher required). Rotate model: drag with left mouse button pressed; shift model: same action+ctrl; zoom: use mouse wheel (or change default action for left mouse button). Select or deselect (or change transparency of) components in the model tree, switch between prefab views, or change surface visualization (e.g. lighting, render mode, crop, etc.)

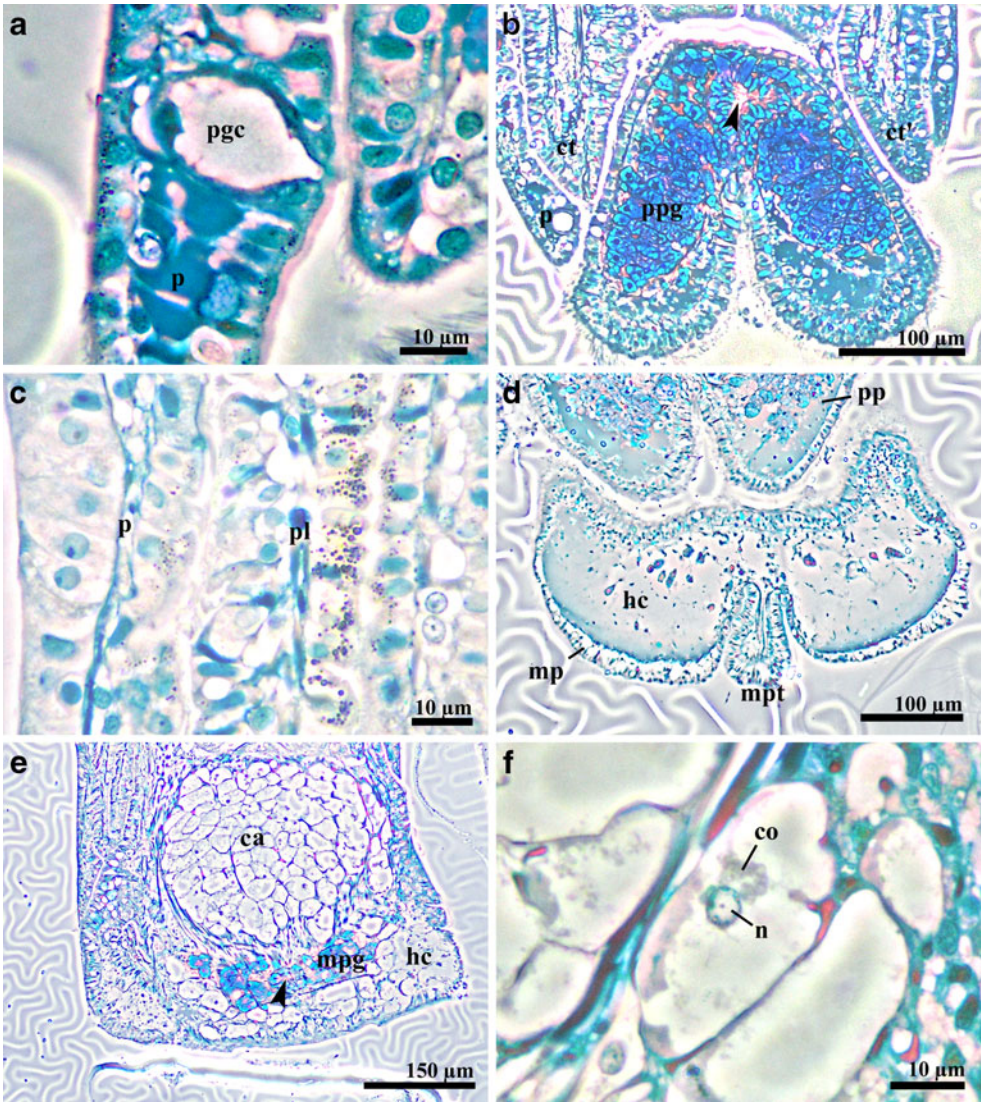

Fig. 3 *Xenoskenea pellucida*, histological details. (**a**) Pallial mucous cells with opening. (**b**) Cross section of propodium with anterior pedal gland (arrowhead: pedal gland duct). (**c**) Longitudinal section of mantle and pallial lobe, the latter showing specific granules in the apical cells. (**d**) Cross section of metapodium with metapodial tentacle. (**e**) Cross section of metapodium with posterior pedal gland (arrowhead: releasing duct) and large mass of calcium cells. (**f**) Detail of calcium cell with small nucleus and concrements. Labels: ca = calcium cells, co = concrements of calcium cells, ct/ct' = right/left cephalic tentacle, hc = haemocoel, mp = metapodium, mpg = metapodial (posterior) pedal gland, mpt = metapodial tentacle, n = nucleus of calcium cell, p = mantle, pgc = pallial glandular cell, pl = pallial lobe, pp = propodium, ppg = propodial (anterior) pedal gland

Main muscles and haemocoel

The columellar muscle runs ventrally along the columella backwards, its right portion is thicker than the left one. The adhesion area is situated near the posterior loop of the intestine. Specific mucle fibres enter the mantle pad and the gill up to the tip, the latter has another retractor from the gill axis to the left mantle (Fig. 2d,e).

The haemocoel shows typical collagen fibers, amoebocytes, and muscles fibers between haemocoelic spaces. So-called rhogocytes (or pore cells) are found scattered throughout the animal's haemocoel. These are characterized by their large size (40 µm×30 µm), oval shape, by a large nucleus and many distinct dark granules in their cytoplasm.

Mantle cavity (Fig. 2)

The epithelial cells of the mantle cavity are characterized by many very small granules, which stain heavily and are concentrated in the distal part of each cell. Such cells are also found at the outer epithelium of the mantle pad. The entire mantle roof includes large blood sinuses, which are separated from each other by fine fibers of muscle or collagen. The mantle cavity itself is quite short, but forms a narrow, deep cleft far backwards on the left side.

The arrangement of the organs of the mantle cavity is unusual (Fig. 2a–c): to the very left, the osphradium forms a short (140 µm), longitudinal ridge that is underlain by the osphradial ganglion. The central anterior roof and the main volume of the mantle cavity are occupied by the single, bipectinate gill. A single, large kidney is situated at the posterior left mantle roof along the efferent sinus of the gill. Behind the kidney the heart is situated. The central and right pallial roof is occupied by the rectal loop. The distalmost portion of the rectum is covered by a very high glandular epithelium. Posteriorly the left digestive gland occupies the central mantle roof. In one individual the vas deferens was swollen and occupied the posterior right

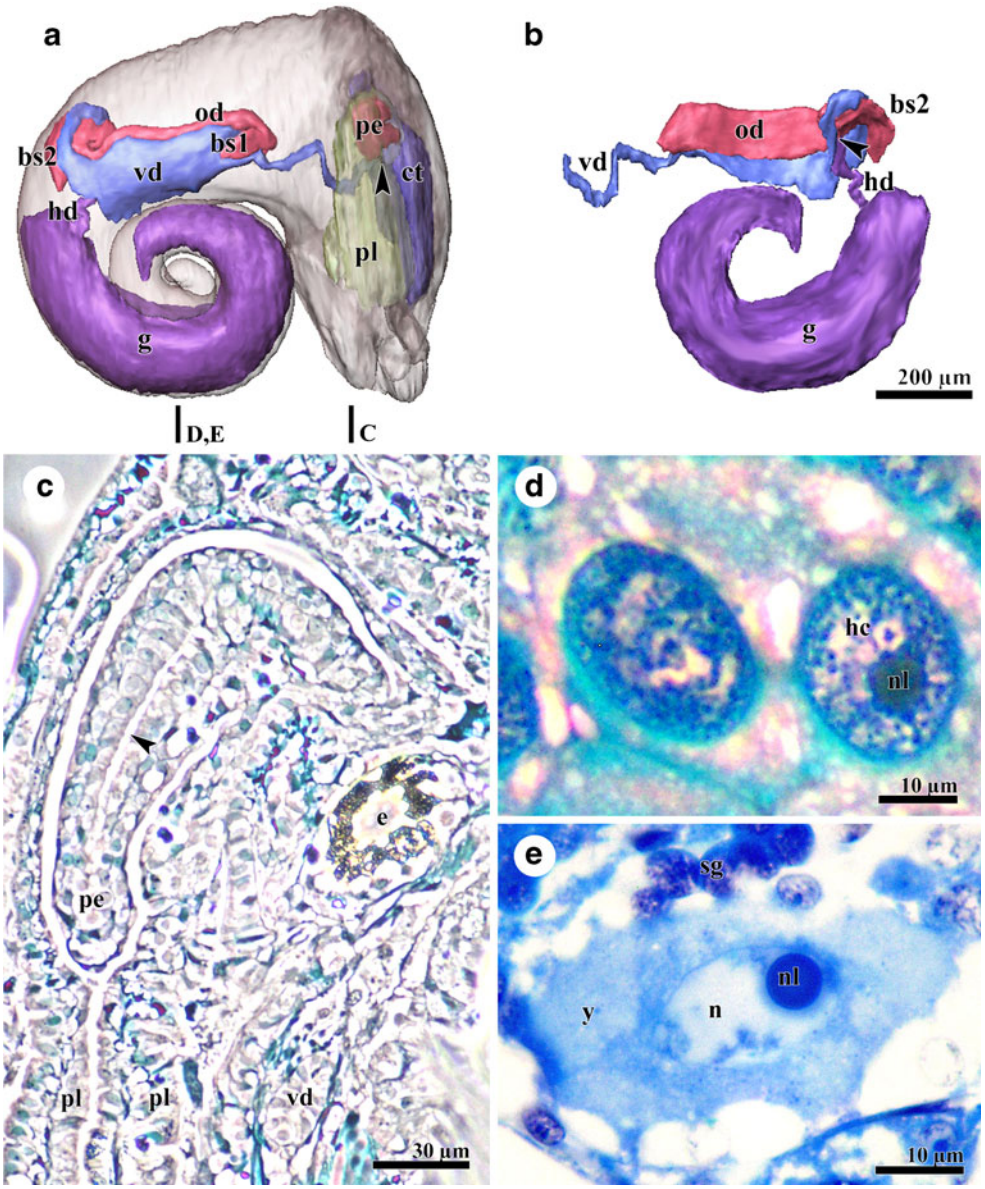

Fig. 4 *Xenoskenea pellucida.* **a**, **b** Reconstruction of genital system; (**a**) right side view, body wall transparent, vertical lines at bottom indicate section planes c–e, arrowhead points to male genital opening; (**b**) left side view, body wall omitted. (**c**) Cross section of anterior vas deferens and penis (longitudinally sectioned) flanked by pallial lobe; arrowhead points to distalmost vas deferens within copulatory organ. (**d**) Detail of thickened part of vas deferens with large nuclei. (**e**) Detail of egg in cross section. Labels: bs1/2 = blind sac 1/2, ct = right cephalic tentacle, e = eye, g = gonad, hc = heterochromatine, hd = hermaphroditic duct, n = nucleus, nl = nucleolus, od = oviduct, pe = penis, pl = pallial lobe, sg = spermatogonia, vd = vas deferens, y = yolk mass

mantle roof, otherwise true pallial gonoducts are lacking. In the retracted animals the mantle pad lies within the anterior right mantle cavity.

The position, special arrangement and structure of the gill (about 0.3 mm long) reflects typical ectobranch (valvatoid conditions) (Fig. 2e,f): Most anteriorly the afferent axis lies dorsally and the efferent axis is situated ventrally. The main retractor muscle is present in the afferent axis. Towards posterior the axis of the gill successively rotates to the left. At the line of the anterior loop of the rectum the main axis forms a transverse sail with the afferent axis to the right and the efferent axis to the left. Shortly posterior the afferent and efferent axes are connected with the mantle roof. Here the gill nerve enters the efferent axis, the afferent sinus is situated to the right of the rectum. The retractor muscle of the afferent axis runs further backwards and is fused posteriorly with the shell muscle. The axes of gill and leaflets are provided with large blood sinuses and thick muscles, whereas skeletal rods and bursicles are lacking. Up to 20 gill leaflets are arranged alternately, their epithelium is densely ciliated on one side and non-ciliated on the other.

Excretory organ, heart and circulatory system (Fig. 2)

A large (diameter 30 µm) afferent gill sinus collects the blood from lacunes of the posterior and ventral visceral hump and enters the afferent (right) gill axis. After passing the lacunes of the leaflets the efferent sinus is formed on the left side, exits the gill towards posterior and becomes the afferent sinus of the kidney (Fig. 2c,f). Leaving the kidney posteriorly the sinus opens into the auricle (diameter about 140 µm), followed by the thick ventricle (90 µm×80 µm). Accordingly,

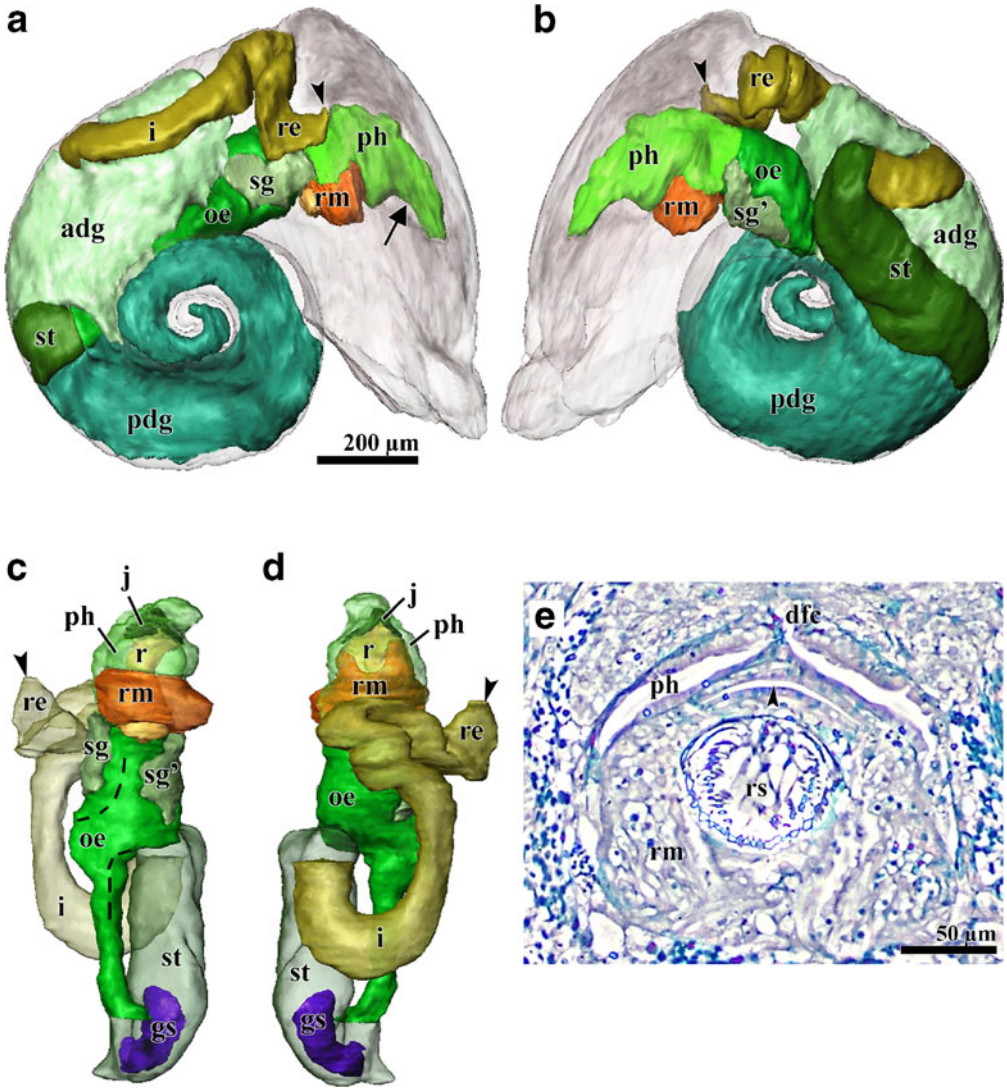

Fig. 5 *Xenoskenea pellucida*, alimentary tract. **a**–**d** Reconstruction of gut anatomy (*arrow*: mouth opening, *arrowheads*: anal opening); (**a**) right side view, body wall transparent; (**b**) left side view, body wall transparent; (**c**) ventral view, dotted lines mark anterio-ventral (*upper line*) and posterio-dorsal midline (*lower line*) of oesophagus during torsion, stomach shown transparent; (**d**) dorsal view, stomach transparent. (**e**) Histological cross section of posterior pharynx (arrowhead: radula caecum). Labels: adg = anterior digestive gland, dfc = dorsal food channel, gs = gastric shield, i = intestine, j = jaw, oe = oesophagus, pdg = posterior digestive gland, ph = pharynx, r = radula, re = rectum, rm = radular musculature, rs = radular sheath, sg/sg' = right/left salivary gland, st = stomach

there is a monotocardian heart. The head aorta runs forwards along the floor of the cephalic haemocoel at midline.

The single, large (260 µm long) kidney of *Xenoskenea pellucida* is solely situated in the mantle roof, its ventral (pallial) wall is equipped with a dense net of blood sinuses. The kidney opening (nephropore) lies posteriorly and is provided with a distinct sphincter muscle. Posteriorly an about 60 µm long, ciliated renopericardial duct connects the kidney dorsally with the pericardium.

Genital system (Fig. 4)

The hermaphroditic gonad occupies the right half of the viscera (Fig. 4a,b). In the central and posterior part of the gonad all stages of spermiogenesis are found. Ripe sperm are filiform, paraspermatozoa could not be detected. Mostly anteriorly there are few, relatively small eggs (diameter 50 µm), which contain yolk granules in their cytoplasm (Fig. 4e). The hermaphroditic duct has a cuboidal epithelium and runs forwards at the very right side of the visceral body. In ripe animals it acts as a seminal vesicle and contains numerous filiform sperm cells. After a short distance (about 100 µm) the hermaphroditic duct splits into an oviduct and a vas deferens.

After the split from the hermaphroditic duct a narrow duct (vas deferens) with cuboidal, ciliated cells runs backwards a short distance, then makes a sharp loop in surrounding the posterior oviduct and runs forwards again along the oviduct. The epithelium of the latter part consists

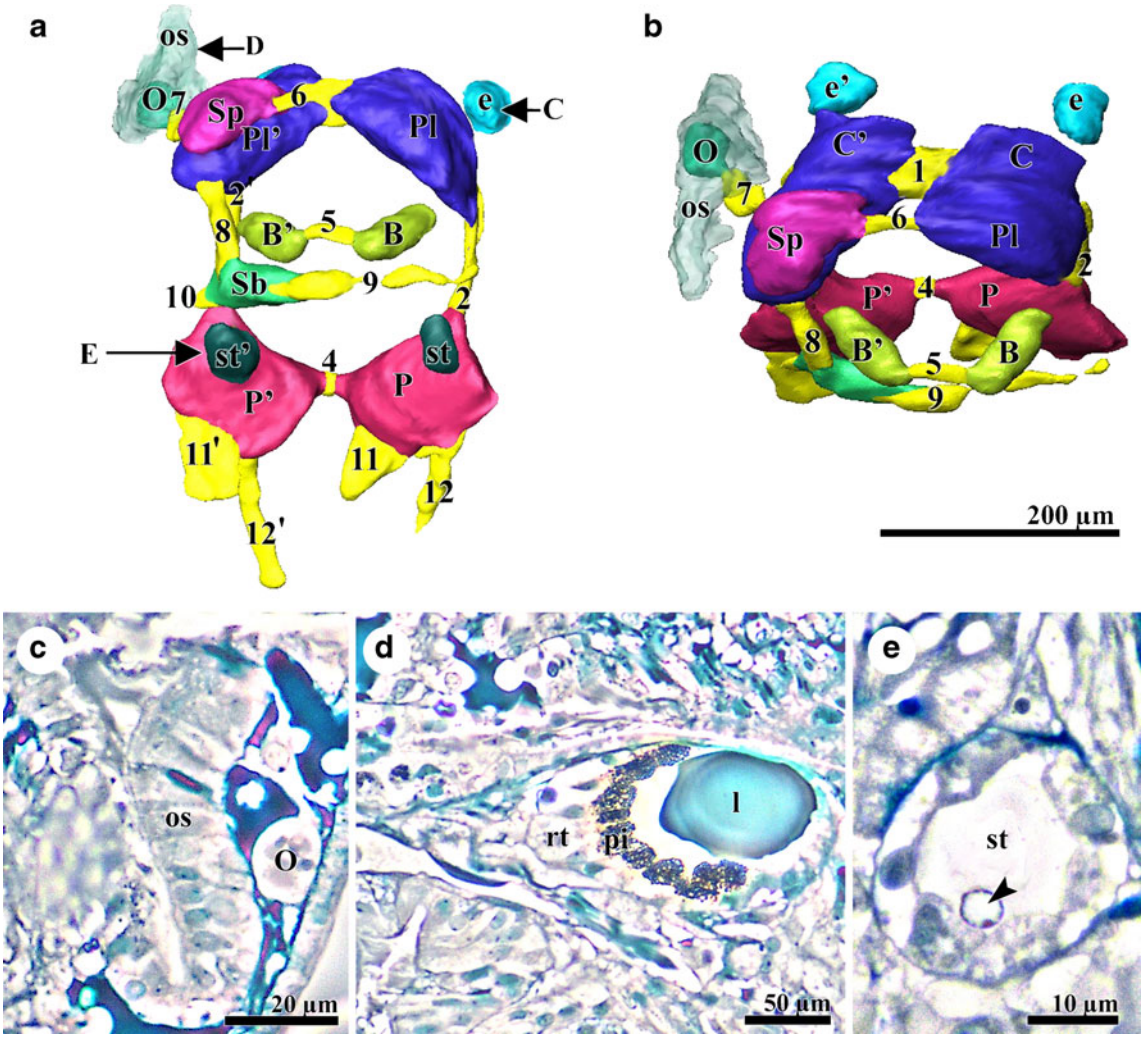

Fig. 6 *Xenoskenea pellucida*, nervous system and sensory organs. **a**, **b** Reconstruction of anatomy of nervous system; (**a**) posterior view, arrows indicate section planes **c**–**e**; (**b**) posterio-dorsal view. **c**–**e** Semithin cross sections showing histological details of sensory organs; (**c**) osphradium, (**d**) eye, (**e**) statocyst, arrowhead points to statolith. Labels: B/B' = right/left buccal ganglion, C/C' = right/left cerebral ganglion, e/e' = right/left eye, l = lense of eye, O = osphradial ganglion, os = osphradial epithelium, P/P' = right/left pedal ganglion, pi: pigments cells, Pl/Pl' = right/left pleural ganglion, rt = retinal cells, st/st' = right/left statocyst, Sb = suboesophageal ganglion, Sp = supraoesophageal ganglion; 1 = cerebral commissure, 2 = cerebropedal connective, 4 = pedal commissure, 5 = buccal commissure, 6 = supraoesophageal connective, 7 = supraoesophageal-osphradial connective, 8 = suboesophageal connective, 9 = mantle nerve, 10 = start of posterior visceral loop (could not be fully reconstructed), 11/11' = right/left anterior pedal nerve, 12/12' = right/left posterior pedal nerve

of highly characteristic, large (diameter 12 µm) cells with big (diameter 8 µm) nuclei and many dense granules of heterochromatine. In ripe animals the distal vas deferens was found to be largely swollen, occupying the anterior visceral body as well as the right posterior mantle roof. At the posterior end of the mantle cavity, the vas deferens forms a small blind sac and is continued abruptly by a much thinner duct, which enters the base of the mantle cavity on the right side and continues forwards along the right neck up to the region of the right eye. In the contracted individuals investigated the vas deferens forms some short, narrow loops, which are probably not present in expanded animals. Most anteriorly the vas deferens shows a small loop around the right eye, enters the base of the small copulatory organ, opening at its tip via a small pore (Fig. 4c). The small and inconspicuous copulatory organ is situated immediately posterior of the right eye (Fig. 1; see also Warén et al. 1993). Throughout its course the vas deferens is a narrow duct (lumen diameter: 15 µm) consisting of cuboidal, ciliated cells (Fig. 4c: vd).

The epithelium of the oviduct is constant throughout and is composed of cuboidal, ciliated cells; there are no special glands or vesicles. The proximal part of the oviduct shows several narrow loops in the right anterior part of the visceral body and forms two small pouches (Fig. 4a,b: bs2) of unknown function. Then the oviduct continues forwards

and its distal part envelops the distal vas deferens to some degree. The small female genital opening is situated at the very posterior right end of the mantle cavity. Immediately before the opening another flat blind sac is orientated backwards, occupying the outer right side of the vas deferens (Fig. 4a,b: bs1). A receptaculum seminis is lacking. The oviduct also acts as a vaginal duct: in one animal a huge spermatophore was found in the oviduct.

Alimentary tract (Fig. 5)

The narrow mouth opening is situated at the tip of the conical snout. There are paired, prominent jaws, which consist of tooth-like elements forming two lateral plates. The buccal cavity is small, there is no sublingual pouch or subradular organ. There is no trace of true radular cartilages, the buccal mass comprises only muscles, connective tissue (fibroblasts) and small parenchymous cells (Fig. 5e: rm). A rhipidoglossate radula (see above for details) with a short (35 μm×70 μm) but distinct radular caecum is present. The radula sheath is very short (200 μm) and straight, at its end there are many small odontoblasts. From the end of the radular sheath two thin but distinct muscles run backwards on the left and right of the oesophagus, accompanying the salivary glands.

The paired salivary glands form thick tubes which run along the oesophagus backwards up to the line of the posterior end of the mantle cavity. Whereas the lumen is extremely narrow, the glandular epithelium consists of large (diameter 14 μm) cells with very large (diameter 8 μm) nuclei. The salivary ducts are very narrow and enter the buccal cavity via a very small pore posterior to the cerebropedal nervous ring.

The buccal cavity is small; an area of mucous cells covers the anterior dorsal wall. Additional mucous areas are found posteriorly at the dorsolateral walls. More posteriorly a prominent dorsal food channel is formed by two large, ciliated folds (Fig. 5e), which continue into the anterior oesophagus. The anterior oesophagus is a wide tube (diameter 170 μm), runs straight backwards, and is accompanied laterally by the two salivary glands and the paired muscles from the radula sheath. The food channel is densely ciliated, whereas the ventral half of the tube lacks cilia. The lateral epithelium contains solitary mucous cells, whereas distinct oesophageal glands or pouches are lacking. At the line of the posterior end of the mantle cavity the oesophagus shows the effect of torsion, the continuing posterior oesophagus is much thinner (diameter 60 μm) and is additionally characterized by complete lack of mucous cells and many, densely ciliated, longitudinal folds. The posterior oesophagus runs backwards into the visceral body, then turns dorsally and enters the stomach just behind the openings of the two digestive glands. The latter occupy the posterior mantle roof as well as the left part of the visceral body (Fig. 5a,b).

The stomach (600 μm×125 μm) is situated at the anterior left visceral wall. It is provided with a prominent gastric shield with tooth and a small caecum (Fig. 5c,d); also a densely ciliated zone is present towards the intestinal region. The ciliated intestine is quite short. Immediately behind the posterior end of the mantle cavity the intestine forms a short 'S', then crosses to the central region to be continued by the rectum, which bypasses the heart. The pallial rectum continues forwards along the central mantle roof, then makes a sharp loop and runs backwards again along the very right mantle roof, separating a distinct mantle channel (Fig. 5d). The anus is situated far posterior in the mantle cavity.

The stomach, intestine and rectum contain detritus and remnants of foraminiferan tests.

Nervous system (Fig. 6a,b)

The nervous system appears as somewhat concentrated due to the small size of the animal, but all ganglia are clearly separated. The cerebral ganglia are situated behind the eyes and are connected by a short commissure (Fig. 6b: 1). The cerebropedal ring is epiathroid; the pleural ganglia are completely fused with the cerebral ones, but both the cerebropedal and the pleuropedal connective are still present. The buccal ganglia are situated at some distance behind the emergence point of the oesophagus and behind the crossing of the visceral loop. The buccal ganglia are connected by a short commissure, their connectives are very thin, their origin marks the posterior ventral end of the cerebral ganglia. The pedal ganglia are connected by a single, short commissure (Fig. 6a, b: 4); there are no pedal cords. A pair of thick anterior nerves supplies the anterior portion of the foot with the anterior pedal gland, a pair of posterior nerves runs into the foot sole and the opercular region. The visceral loop is streptoneurous, the supraoesophageal ganglion contacts the left pleural ganglion dorsally (Fig. 6a,b), but there is no zygoneurous connective. From the supraoesophageal ganglion a thick connective (Fig. 6a,b: 7) runs forwards to the left, enters the left mantle roof and swells to a distinct osphradial ganglion, which supplies the osphradium, the gill and the left mantle margin. The suboesophageal ganglion lies ventrally to the left; a thick mantle nerve (Fig. 6a: 9) emerges from it and runs below the oesophagus to the right mantle margin. The posterior part of the visceral loop is long and very inconspicuous; the connectives run within the shell muscle. No visceral or genital ganglion was detected.

Sensory organs (Fig. 6c–e)

The cephalic tentacles lack sensory papillae, but there is a distinct ciliated zone on the dorsal inner side. The histology changes from proximal to distal: The basalmost epithelium resembles that of the mantle cavity (see above). At

midlength the epithelium consists of cuboidal, poorly stained mucous cells with round nuclei, which are separated by groups of 3–4 very narrow (20 μm×3 μm) supporting cells. Near the tip the epithelium is composed of supporting cells characterized by oval nuclei, whereas sensory cells have round nuclei which are situated more basally. The longitudinal retractor muscles are arranged in several bundles, together with transversal fibers they form a muscular hydrostat (cf. Marshall and Hodgson 1990). A single, prominent blood sinus is situated dorsally. The tentacle nerves emerge from the outer anterior side of the cerebral ganglia and bifurcate at the basis of the tentacle after a short distance.

The ridge-like osphradium is supplied by the prominent, underlying osphradial ganglion; the central sensory epithelium consists of ciliated cells flanked by non-ciliated lateral zones (Fig. 6c).

At the outer base of the cephalic tentacles there are well-developed, closed eyes (diameter 50 μm) with a concentrically layered lens and distinct pigment cells (Fig. 6d). The optical nerves emerge near the anterior end of the cerebral ganglion.

The small (50 μm×35 μm×17 μm) statocysts are situated at the posterior median wall of the pedal ganglia. Each of them contains a single, small (diameter 6 μm) statolith (Fig. 6e).

Available data from other sources

Warén et al. (1993) described the shell as small (max. 2 mm), depressed, and transparent, the smooth protoconch as indistinctly hyperstrophic and with 0.75 whorls (op.cit.: fig. 30). The radula is rhipidoglossate with the formula n − 3 − 1 − 3 − n (op.cit.: SEM figs. 31, 32); more than 25 marginal teeth are present. Drawings of a live animal (op.cit.: figs. 33–36; our Fig. 1) show a long, cylindrical snout with two anterior tentacles. The eyes are well visible and are situated at the median basis of the cephalic tentacles; behind the right eye a small copulatory tentacle is present. On the right side a large mantle pad covers a part of the preceding whorl (Fig. 1: pl), but was fully contracted in our studied specimens. The foot has two anterior lappets and one median posterior tentacle, epipodial tentacles are lacking. A prominent, bipectinate gill may be protruded from the mantle cavity on the right side. We could confirm all these characters and those on external morphology in our specimens studied.

Hyalogyrina depressa **Hasegawa, 1997**

(Figures 7, 8, 9, 10, 11, 12 and 13)

External morphology

The head bears a conical snout with two anterior bulges. The right side of the head and the neck region are densely ciliated, the neck also shows a glandular epithelium. The cephalic tentacles are dorsoventrally flattened. A small (300 μm long), conical pallial tentacle is visible at the right opening of the mantle cavity. This tentacle is densely ciliated (Fig. 8a) and equipped with prominent longitudinal muscle fibers. Eyes and epipodial tentacles are lacking; the mantle margin is smooth and ciliated.

Foot and shell muscles

In the contracted animals the foot is transversely folded like a pocket knife (Fig. 7a,b). The anterior foot is deeply bilobed, the posterior end is rounded. The epithelium of the foot's sole consists of highly cylindrical, densely ciliated cells interspersed with poorly stained mucous cells. The back of the foot lacks cilia, however. The anterior foot gland forms an irregular mass in the dorsal half of the propodium. Two lobes of this mass fill the anterior foot lappets, another two lobes extend laterally, and one lobe runs backwards ventrally. The central duct (diameter 25 μm) opens at the anterior median edge of the foot sole. The cells are large (20 μm× 36 μm) and have irregularly shaped, basal nuclei (Fig. 7e).

The much smaller, posterior foot gland contains weakly stained mucous cells and opens via a short duct in the center of the foot sole. The posterior gland forms a flat mass and is somewhat embedded in the connective tissue of the foot.

In the central portion of the foot there is an accumulation of very large (diameter 60–95 μm), clear, oval to deformed calcium cells with large (diameter 15 μm), round nuclei. Whereas the cytoplasm of these cells is restricted to narrow strings, the main volume of the cells is mainly occupied by large vacuoles containing fine concrements (Fig. 7d), which show negative contrast in phase contrast microscopy. Otherwise the foot mass contains muscle and collagen fibers as usual, haemolymph spaces and parenchymous cells.

There is a single columellar muscle, which adheres ventrally at the shell (Fig. 9a,b).

Mantle cavity (Fig. 7a–c)

The mantle cavity occupies about one third of the volume of the last shell whorl. The anterior part of the mantle cavity is occupied by the gill. On the left side, about 200 μm behind the edge, the osphradium forms a thickened ridge. More posterior and to the left the single kidney is situated in front of the monotocardian heart. The posterior, central and right mantle roof is occupied by several rectal loops, followed towards posterior right by the receptaculum seminis and the gonoduct with the gonopore. The posterior wall of the mantle cavity is formed by the bursa copulatrix, the anterior portion of the digestive gland, and to the left by the stomach.

The whole mantle roof is underlain by wide blood sinuses, in particular near the anterior mantle edge. On the inner side of the mantle roof there are various glands with

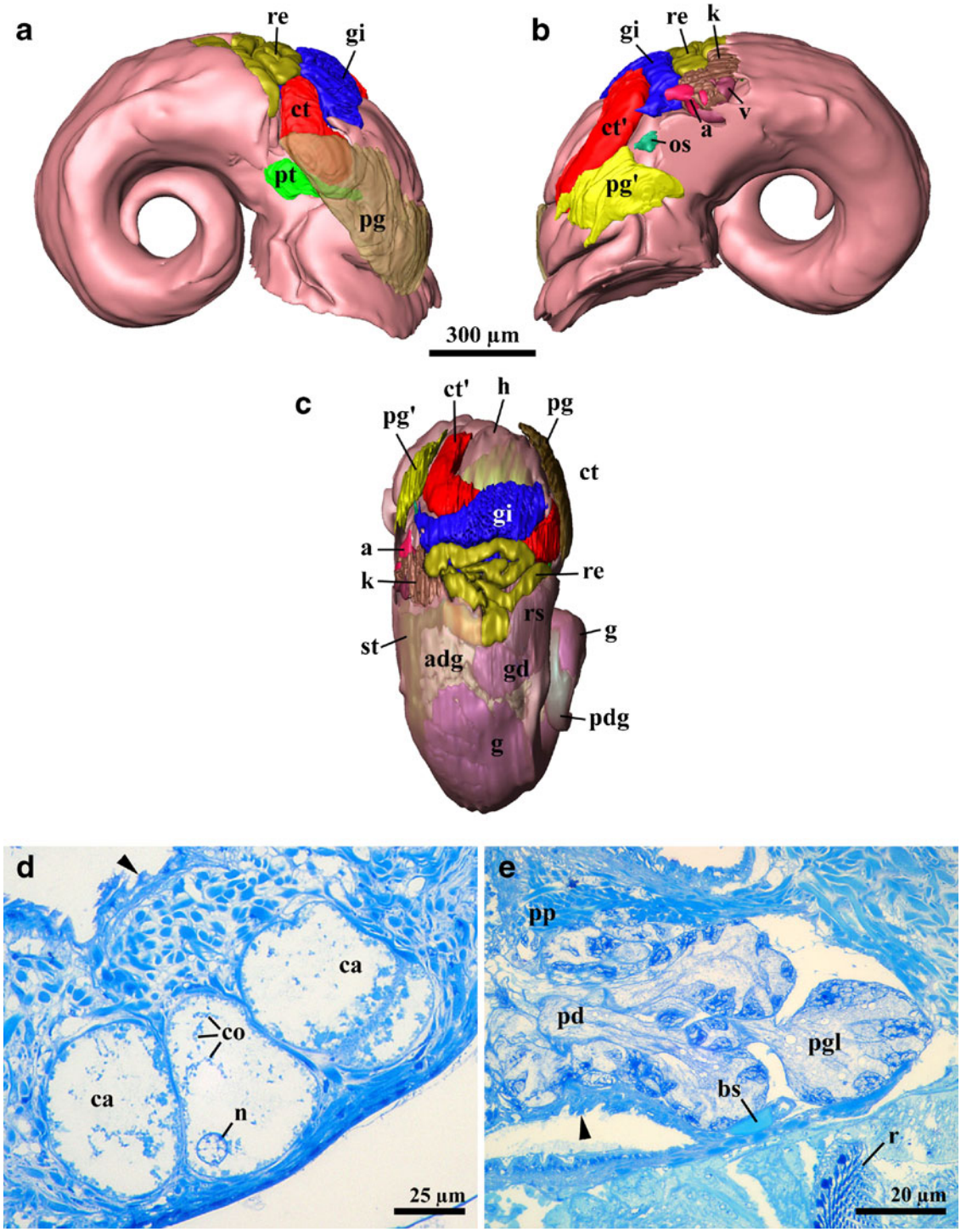

Fig. 7 *Hyalogyrina depressa*. **a**–**c** Reconstructions of mantle cavity, mantle roof omitted, visceral sac transparent in c; (**a**) right side view, (**b**) left side view, (**c**) dorsal view. **d**, **e** Histological details of foot; (**d**) sagittal section of dorsal mesopodial calcium cells (*arrowhead*: foot sole), (**e**) parasagittal section of lobes of anterior foot gland (*arrowhead*: foot sole). Labels: a = auricle, adg = anterior digestive gland, bs = blood sinus, ca = calcium cell, co = concrements of calcium cell, ct/ct' = right/left cephalic tentacle, g = gonad, gd = gonoduct, gi = gill, h = head, k = kidney, n = nucleus, os = osphradium, pd = pedal gland duct, pdg = posterior digestive gland, pg/pg' = right/left pallial glandular area, pgl = pedal gland lobe, pp = propodium, pt = pallial tentacle, r = radula, re = rectum, rs = receptaculum seminis, st = stomach, v = heart ventricle. Supplementary plate 2 offers an interactive 3D model of *Hyalogyrina depressa* that can be accessed by clicking into Fig. 7 (Adobe Reader version 7 or higher required). Rotate model: drag with left mouse button pressed; shift model: same action+ctrl; zoom: use mouse wheel (or change default action for left mouse button). Select or deselect (or change transparency of) components in the model tree, switch between prefab views, or change surface visualization (e.g. lighting, render mode, crop, etc.)

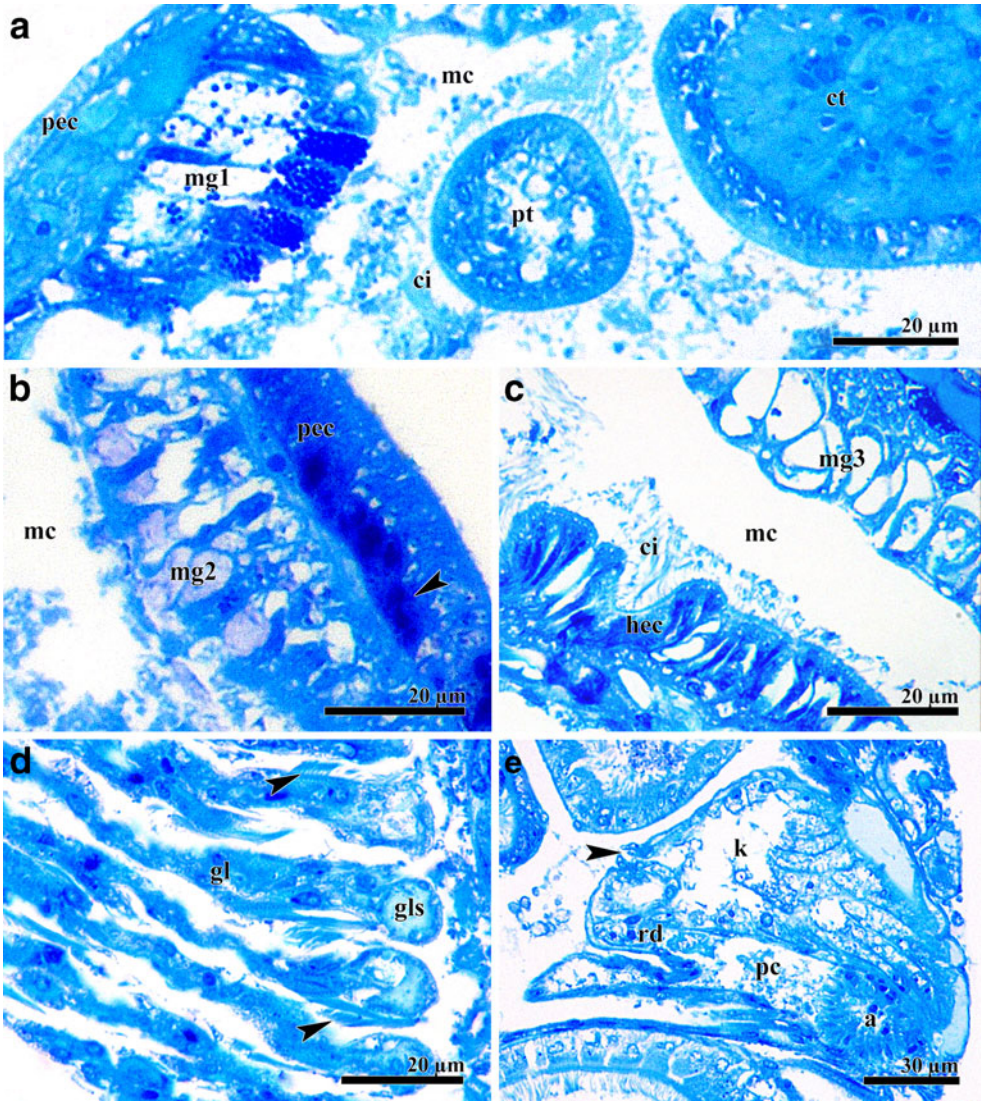

Fig. 8 *Hyalogyrina depressa*, histological details of mantle cavity (semithin sections). (**a**) Cross section of right anterior mantle cavity. (**b**) Cross section of left mantle roof (*arrowhead*: dark glandular components). (**c**) Cross section of median mantle roof opposed to ciliated neck. (**d**) Longitudinal section of gill lamellae (*arrowheads*: lateral cilia). (**e**) Cross section of left kidney with heart (arrowhead: nephropore). Labels: a = auricle of heart, ci = cilia, ct = right cephalic tentacle, gl = gill lamellae, gls = efferent sinus of gill lamellae, hec = epidermis of head, k = kidney, mc = mantle cavity, mg1/2/3 = pallial mucous cell of type 1/2/3, pc = pericardium, pec = pallial epidermis, pt = pallial tentacle, rd = renopericardial duct

various types of mucous cells: the right pallial gland consists of cells with an empty or bubble-like structure, and occasional dark, apical granules dominate (Fig. 7a: pg; 8a: mg1). On the left side another pallial gland has mucous cells showing metachromatic content (Fig. 7b: pg'; 8b: mg2). In the central pallial roof and occasionally also laterally there are mucous cells which appear empty in the sections (Fig. 8c: mg3).

The bipectinate gill shows about 20 alternating lamellae, which have ciliary tracts and regions with very flat (respiratory) epithelia (Fig. 8d). Beneath the efferent blood sinus, the efferent gill axis has a thick muscle which runs into the left mantle, but on the right (afferent) side no distinct retractor is present.

Excretory organ, heart and circulatory system (Fig. 9)

The rectal sinus runs along the rectum forwards to the right and enters the afferent axis of the gill. After passing the leaflets the efferent gill sinus collects the haemolymph and also receives a mantle sinus, thus becoming the afferent sinus of the kidney. After passing the kidney walls the efferent kidney sinus opens into the auricle, followed by the ventricle (Fig. 9b,c). The head aorta runs forwards along the median mantle floor.

The monotocardian heart is situated in the left posterior mantle cavity. The kidney forms a boomerang-shaped organ in the posterior mantle roof and shows a distinct nephropore (Fig. 8e: arrowhead). It is connected with the pericardium by a ciliated renopericardial duct.

Genital system (Figs. 10, 11)

The true hermaphroditic gland occupies the right half of the visceral body (Fig. 10a). The right portion has a homogenous lumen, from which several lobes expand to the left (Fig. 10b,c). The inner portion of these lobes produces the eggs, which become more mature from left to right and from posterior to anterior (Fig. 11f). Spermiogenesis takes

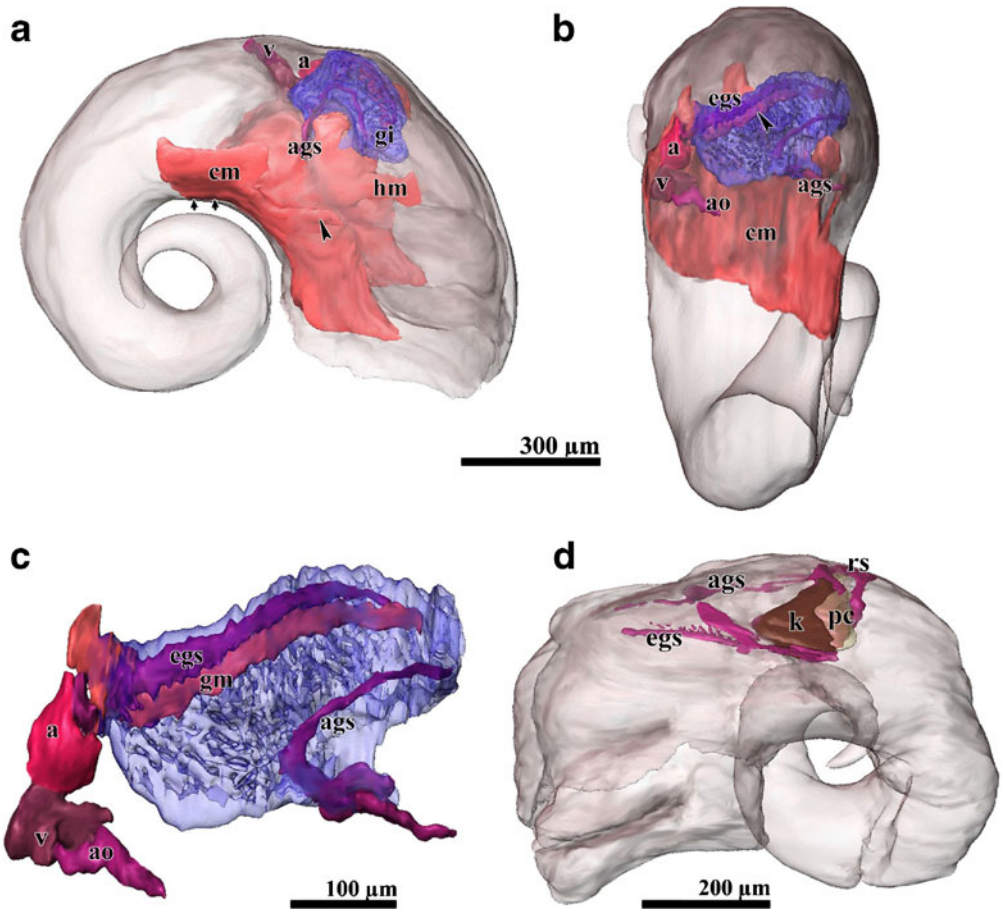

Fig. 9 *Hyalogyrina depressa*, reconstruction of muscles, circulatory and excretory system. (**a**) Right side view, body shown transparent (*arrowhead*: muscle of pallial tentacle, *small arrows*: adhesive zone of columellar muscles). (**b**) Dorsal view, body transparent (*arrowhead*: gill muscle). (**c**) Detail: gill in dorsal view with afferent and efferent sinuses and gill muscle. (**d**) Circulatory system and kidney (pericardium transparent), left side view. Labels: a = auricle, ags = afferent gill sinus, ao = aorta, cm = columellar muscle, egs = efferent gill sinus, gi = gill, gm = gill muscle (retractor), hm = head muscle (retractor), k = kidney, pc = pericardium, rs = rectal sinus, v = heart ventricle

place towards the central parts in the portions of the hermaphroditic gland which lie adjacent to the external epithelium of the visceral sac (Fig. 11f). Mature sperm (only one type is present) have filiform heads and long flagella, and are orientated centrifugally (Fig. 11g).

The hermaphroditic duct emerges on the median side of the gonad and runs to the right, where it widens to form a vesicula seminalis containing autosperm with their heads orientated forwards (Fig. 11d). From the proximal part of the gonoduct a prominent blind sac (ca. 350×100×40 µm) emerges ventrally (Figs. 10a,b; 21c: vs). Its dorsal epithelium consists of thick (up to 22 µm) glandular cells with heavily stained cytoplasms, whereas the ventral epithelium is densely ciliated. The gonoduct as a whole forms an S-shaped loop towards ventral, then anteriorly left, and finally runs in a curve to ventral right towards the genital atrium. It consists of three histologically distinct regions (Fig. 10d: gd1/2/3), as follows. (1) The glandular proximal part shows many dark granules of various sizes, further structures are poorly preserved (Fig. 10d: gd1). From here a prominent (350 µm×100 µm×40 µm) blind sac emerges (Figs. 10d; 11a: bs1). Its epithelium shows mucous cells with dark cytoplasm and pale nuclei, as well as clear granula or vesicles; the ventral epithelium is densely ciliated. (2) The proximal part is continued by the central part of the gonoduct consisting of long, ciliary cells filled with large, dark vesicles (Figs. 10d; 11a,c: gd2). At the distal end of the central part another glandular blind sac (440 µm× 95 µm×30 µm) is formed, somewhat surrounding the gonoduct (Figs. 10d; 11a: bs2). This gland consists of many lobes with lightish, homogeneous lumina; the lumen opens via a ciliary duct into the gonoduct. (3) The distalmost part of the gonoduct is again formed by long cells with granules, but the latter show metachromic staining (Fig. 11a: gd3). The duct finally enters the genital atrium, from which the following two further structures arise.

(A) The bursa copulatrix is embedded in the proximal and median gonoduct (Fig. 10b,c). It is a bean-shaped structure (50 µm×160 µm×50 µm) with a ciliated

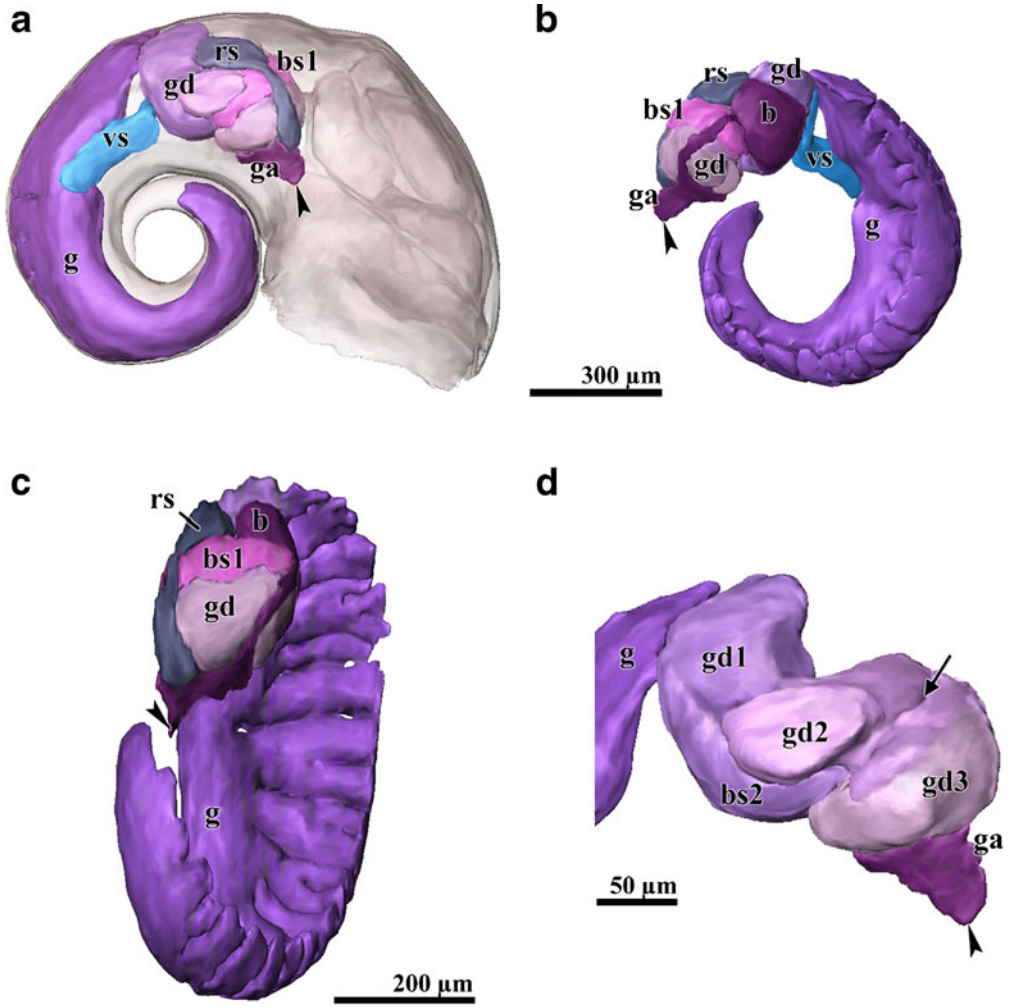

Fig. 10 *Hyalogyrina depressa*, reconstruction of genital system, arrowheads mark opening of genital atrium into mantle cavity. (**a**) Right side view, body shown transparent. (**b**) Left side view, body wall omitted. (**c**) Frontal view. (**d**) Right side view, detail of various parts of gonoduct (*arrow marks* position of blind sac 2 along ridge). Labels: b = bursa, bs1/2 = blind sac 1/2, g = gonad, ga = genital atrium, gd = gonoduct, gd1/2/3 = proximal/median/distal portion of gonoduct, rs = receptaculum seminalis, vs = ventral sac

epithelium. Its large lumen shows organic particles that could not be identified unequivocally, but probably are degraded allosperm (Fig. 11e). A narrow, ciliated duct connects the bursa with the genital atrium.

(B) The receptaculum seminis (160 µm×80 µm×70 µm) is situated to the right of the bursa and also lies adjacent to the gonoduct (Fig. 10a–c: rs). It is filled with densely packed allosperm (Fig. 11c). The ciliated duct runs along the gonoduct and again opens into the genital atrium.

The genital atrium itself opens via a short duct into the posterior right mantle cavity. A copulatory organ is not present.

Alimentary tract (Fig. 12)

The small and narrow mouth opening is flanked by lateral oral lappets. Behind the mouth opening two triangular jaw plates are situated laterodorsally, consisting of tooth-like elements flanking the oral cavity, which is of inverted Y-shape (Fig. 12d). The radula is supported by a purely muscular odontophore; true cartilages are lacking. The radula sheath makes a sharp loop downwards, its blind end consists of numerous odontoblasts (Fig. 12e).

The pharynx continues dorsally into the anterior oesophagus, which shows several densely ciliated, longitudinal folds (Fig. 12f). It is flanked by the paired, large (200 µm×80 µm×40 µm) salivary glands, which possess many small lobes. The salivary ducts show many loops (due to the contracted condition), their glandular epithelia are heavily stained, whereas the posterior parts show large, pale cells with very large nuclei (Fig. 12g). Effects of torsion are minimal; the posterior part is a simple, narrow (diameter 55 µm) tube that runs backwards and enters the stomach between the openings of the two digestive glands (Fig. 12i).

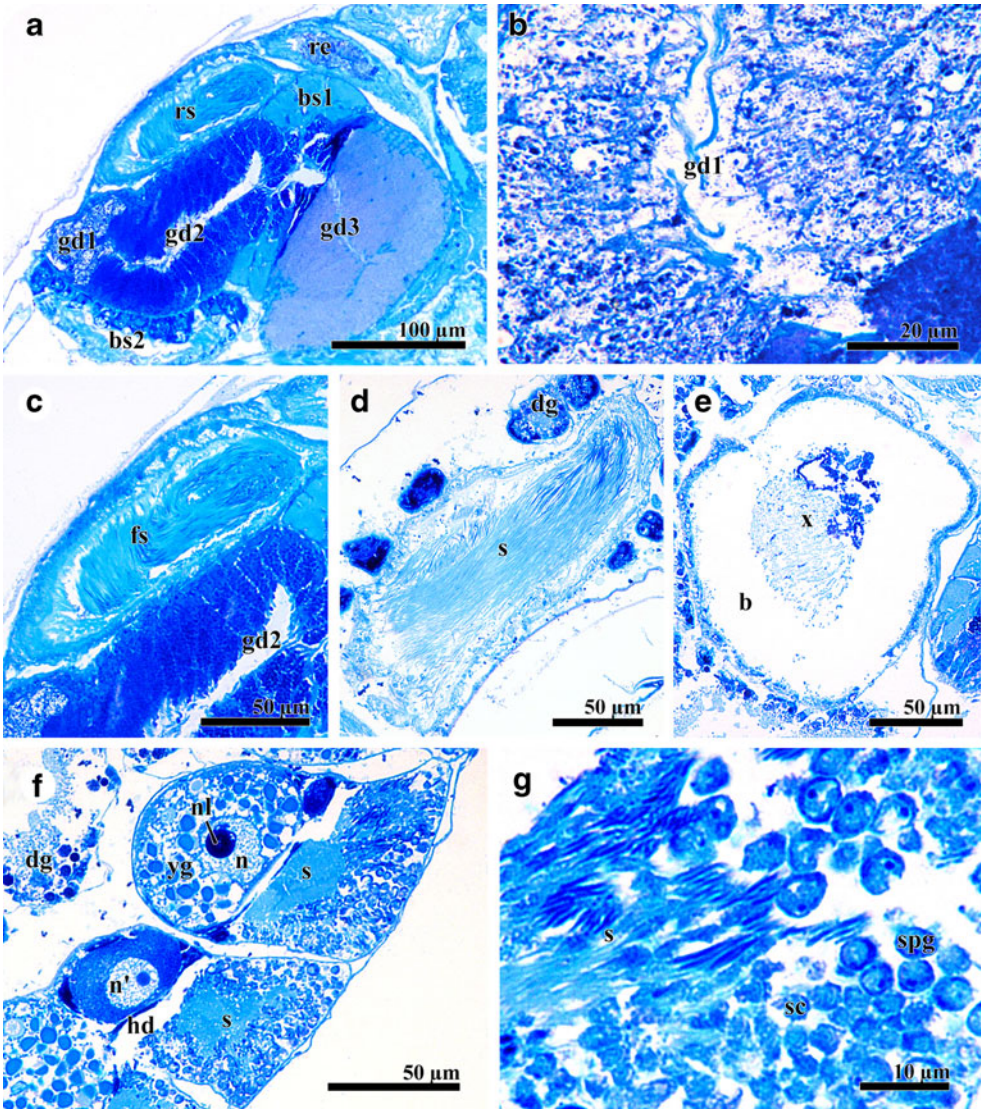

Fig. 11 *Hyalogyrina depressa*, histological details of genital system (semithin sections). (**a**) Overview: longitudinal section of gonoducts and associated structures, anterior is at right. (**b**) Detail: longitudinal section of proximal part of gonoduct. (**c**) Cross section of receptaculum seminis. (**d**) Longitudinal section of vesicula seminalis with autosperm. (**e**) Longitudinal section of bursa copulatrix with degraded allosperm. (**f**) Cross section of ovotestis lobes, each with inner ovary and outer testis portion. (**g**) Detail of f: spermatogenesis in peripheral portion of ovotestis. Labels: b = bursa, bs1/2 = blind sac1/2, dg = digestive gland, fs = allosperm, gd1/2/3 = proximal/median/distal portion of gonoduct, hd = hermaphroditic duct, n/n' = nucleus of ripe/juvenile egg, nl = nucleolus, re = rectum, rs = receptaculum seminis, s = autosperm, sc = spermatocyte, spg = spermatogonium, x = degraded allosperm, yg = yolk granules

The posterior stomach (diameter 500 µm) is equipped with a large but thin gastric shield with tooth, followed more anteriorly by ciliated areas with high prismatic cells (Fig. 12h). Again a small caecum is present at the ventral side of the stomach (Fig. 12h: ca).

The anterior digestive gland occupies the visceral body to the right of the stomach, whereas the posterior gland fills the visceral sac. Both consist of a spreading duct system reaching into irregularly shaped diverticles (Fig. 12i). The epithelium of the digestive glands shows lightish cells with round nuclei and a compact cytoplasm in the apical portion (Fig. 12i).

The short and ciliated intestinal tube (diameter 80 µm) emerges from the stomach on the right side, runs forwards and then upwards entering the mantle roof. The rectal portion shows several narrow loops in the mantle roof (Figs. 7c; 12c). The anal opening is situated in the posterior right mantle cavity.

Stomach and intestine contain remnants of detritus, including diatom tests.

Nervous system (Fig. 13a,b)

The cerebral ganglia are situated at the basis of the cephalic tentacles. They are compressed dorsoventrally and connected by a short commissure. The tentacle nerve bifurcates shortly after emergence (Fig. 13a,b: nerve 2). The pleural ganglia are fused with the cerebral ganglia (epiathroid condition); these cerebropleural ganglia are connected to the pedal ganglia by two connectives (n3, n4). The pedal ganglia are connected by a short commissure; one pair of pedal nerves runs forwards (n6), another pair (n7) backwards into the foot. The buccal ganglia with their thin and quite long commissure (n9) are situated at the line of the opening of the salivary glands, and are connected to the cerebral ganglia (n8).

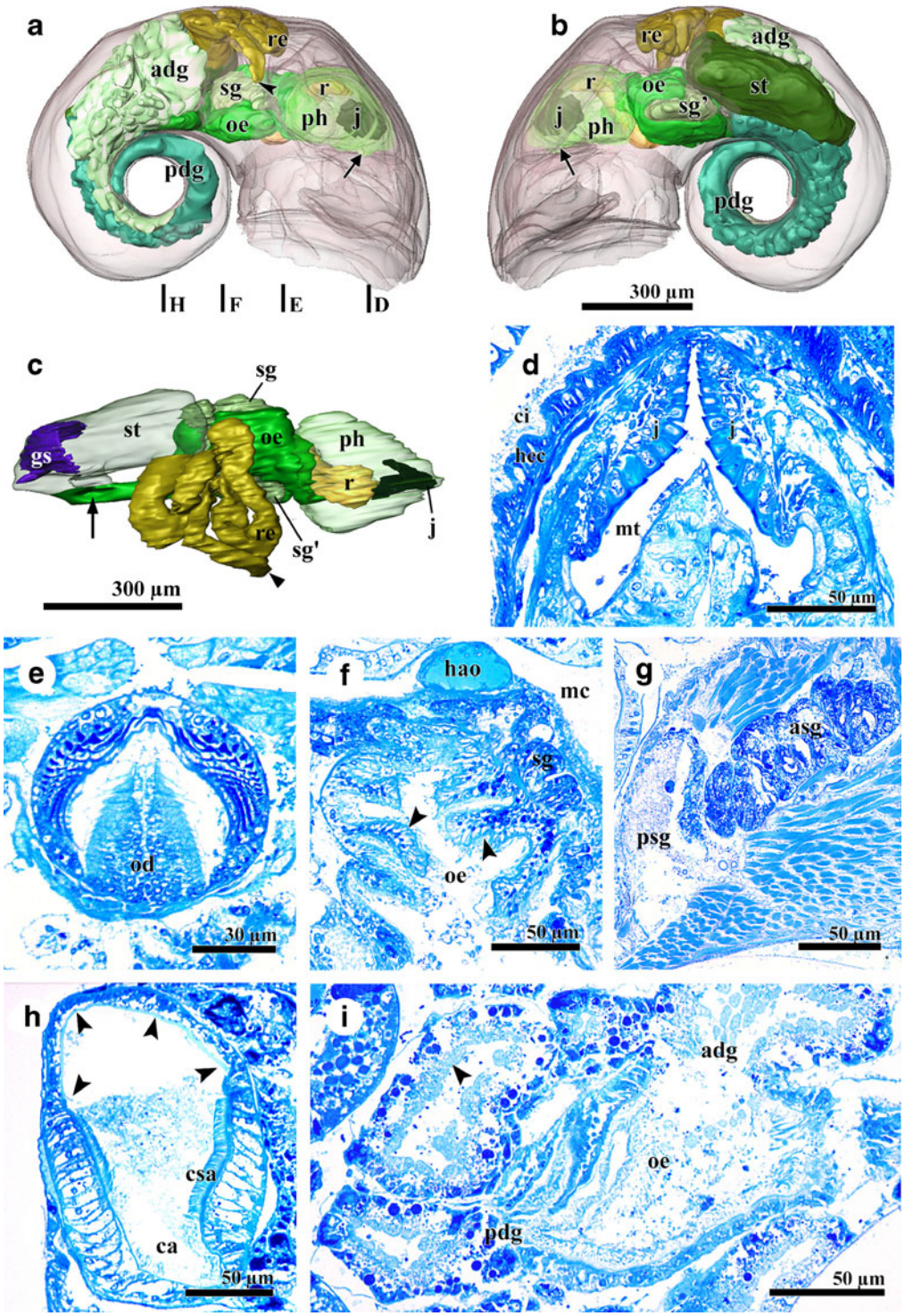

Fig. 12 *Hyalogyrina depressa*, alimentary tract. **a**–**c** Reconstruction of anatomy; (**a**) right side view, body wall shown transparent, vertical lines at bottom indicate cross section planes **d**–**f** and **h** (*arrowhead*: anal opening, arrow: mouth opening); (**b**) left side view, body wall transparent (*arrow*: mouth opening); (**c**) ventral view, pharynx and stomach transparent (*arrowhead*: anal opening, *arrow*: opening of posterior digestive gland). (**d**) Cross section of mouth tube with jaw. (**e**) Cross section of radular sheath. (**f**) Cross section of anterior oesophagus (arrowheads mark folds). (**g**) Longitudinal section of salivary gland, anterior is at right. (**h**) Cross section of posterior stomach (arrowheads: gastric shield). (**i**) Longitudinal section of posterior oesophagus at line of digestive gland openings, anterior is at right (arrowhead: dense cytoplasm of apical epithelium of digestive gland). Labels: adg = anterior digestive gland, asg = anterior part of salivary gland, ca = stomach caecum, ci = ciliary border, csa = ciliary sorting area of stomach, gs = gastric shield, hao = head aorta, hec = head epidermis, j = jaw, mc = mantle cavity, mt = mouth tube, od = odontoblasts, oe = oesophagus, pdg = posterior digestive gland, ph = pharynx, psg = posterior part of salivary gland, r = radula, re = rectum, sg/sg' = right/left salivary gland, st = stomach

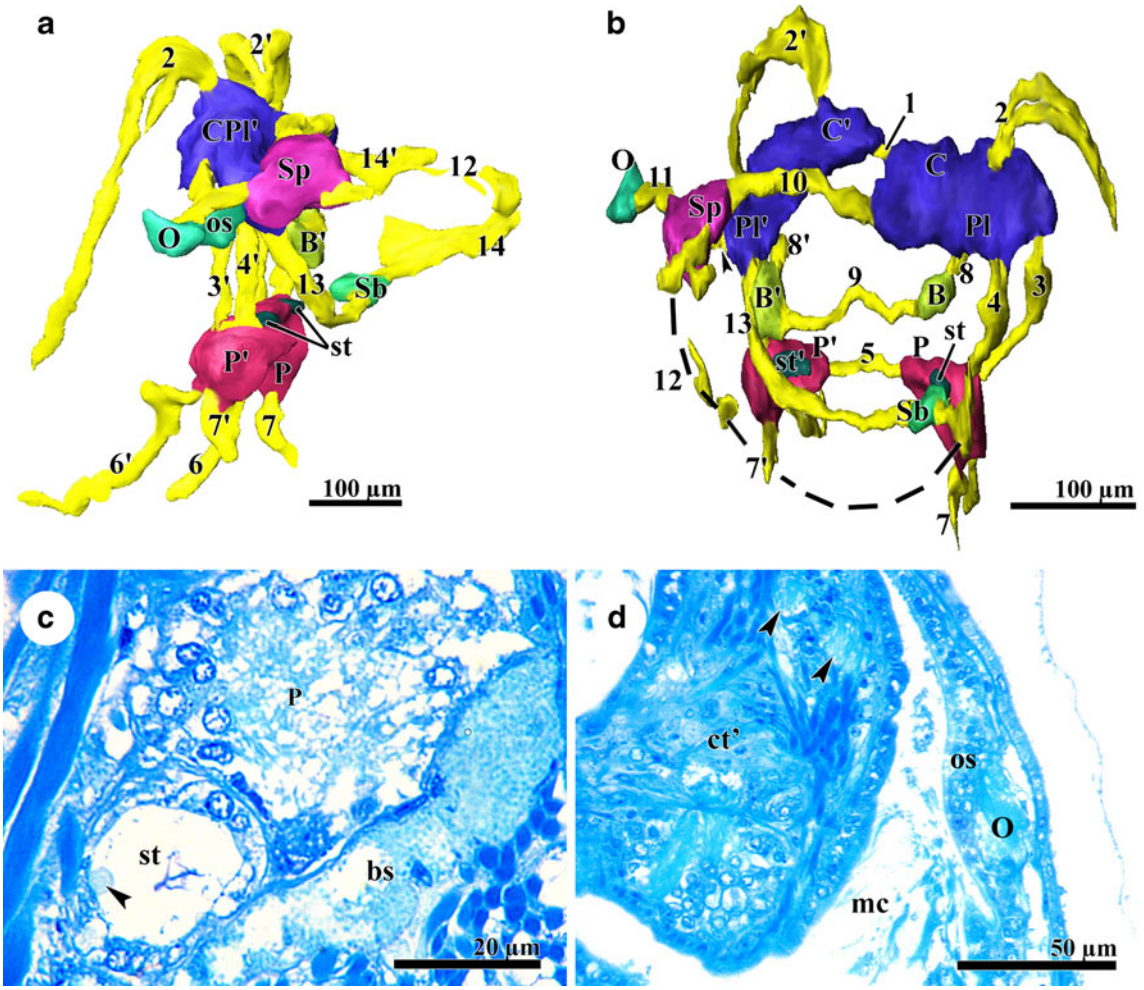

Fig. 13 *Hyalogyrina depressa*, nervous system and sensory organs. **a**, **b** Reconstruction of anatomy of nervous system; (**a**) left side view, (**b**) posterior view: dotted line indicates posterior part of visceral loop which could not be reconstructed (arrowhead: left zygoneurosis). **c**, **d** Histological details of sensory organs (semithin cross sections); (**c**) statocyst (arrowhead: statocone), (**d**) left cephalic tentacle and osphradium (arrowheads: tentacle nerves). Labels: B/B' = right/left buccal ganglion, bs = blood sinus, C/C' = right/left cerebral ganglion, CPl' = left cerebropleural ganglion, ct' = left cephalic tentacle, mc = mantle cavity, O = osphradial ganglion, os = osphradial epithelium, P/P' = right/left pedal ganglion, Pl/Pl' = right/left pleural ganglion, Sb = suboesophageal ganglion, Sp = supraoesophageal ganglion, st/st' = right/left statocyst; 1 = cerebral commissure, 2/2' = right/left tentacle nerve, 3/3' = right/left cerebropedal connective, 4/4' = right/left pleuropedal connective, 5 = pedal commissure, 6/6' = right/left anterior pedal nerve, 7/7' = right/left ventral pedal nerve, 8/8' = right/left cerebrobuccal connective, 9 = buccal commissure, 10 = supraoesophageal connective, 11 = supraoesophageal-osphradial connective, 12 = visceral loop, 13 = suboesophageal connective, 14/14' = right/left mantle nerve

From the right pleural ganglion a connective (n10) crosses above the oesophagus to the left side and reaches the supraoesophageal ganglion, which is situated above the left pleural ganglion. From the latter a short nerve (n11) connects to the osphradial ganglion in the left mantle roof. A left zygoneurosis (Fig. 13b: arrowhead) connects the left pleural with the supraoesophageal ganglion. Posteriorly a mantle nerve (n12) and the posterior portion of the visceral loop (n14') emerge from the left pleural ganglion.

From the left pleural ganglion another connective (n13) crosses below the oesophagus to the right and reaches the suboesophageal ganglion at the line of the right pedal ganglion. Again a mantle nerve (n12) and the posterior part of the visceral loop (n14) emerge posteriorly. A visceral ganglion could not be detected.

Sensory organs (Fig. 13c,d)

Eyes and epipodial tentacles are entirely lacking; the cephalic tentacles are smooth (Fig. 13d). Each of the two bean-shaped statocysts (30 µm×20 µm×10 µm), which are situated at the postero-dorsal sides of the pedal ganglia, contains a small (diameter 12 µm), round statolith (Fig. 13c). The osphradial epithelium is higher than that of the surrounding mantle roof; histological details could not be detected (Fig. 13d).

Data from other sources

Hasegawa (1997) gave SEM images of the depressed, smooth shell (op.cit.: fig. 29A–C), the hyperstrophic granular to smooth protoconch (fig. 29D, E) forming an anastrophic apex, of the round, multispiral operculum (fig. 29F), the rhipidoglossate radula (fig. 29G, H) with the formula n-1-1-1-n, and of a jaw plate (fig. 29I) consisting of tooth-like elements. He also provided SEM photos of the head-foot (fig. 30A, B) and the gill leaflets (fig. 30C).

***Hyalogyrina grasslei* Warén & Bouchet, 1993**
(Figures 14, 15, 16 and 17)

External morphology

The epithelium of the head region is covered by a microvillous border with interspersed ciliary tufts. The snout is tapered but slightly bilobate, the mouth opening is quite small. Between the cephalic tentacles there are two short, ciliated knobs (Fig. 14a,b). Another small process—probably a copulatory organ (see below)—is situated at the basis of the right cephalic tentacle close to the openings of receptaculum and gonoduct. A seminal groove could not be detected. In the anterior part of the right mantle cavity there is another small (about 0.2 mm), ciliated tentacle.

Pedal structures

The foot is folded due to preservation. The single pedal gland opens via a wide pore at the anterior border of the foot, but its posterior portion is difficult to distinguish from the surrounding connective tissue. In the center of the foot there is a densely packed group of large (diameter 80 μm) and transparent calcium cells, each provided with a large (diameter 13 μm) nucleus (Fig. 15g). The remaining foot mass shows large haemocoelic spaces with interspersed collagen and muscle fibers; parenchymous cells are rare.

Shell muscle, haemocoel, and mantle cavity

The conditions of the shell (columellar) muscle and of the haemocoel resemble those in *Xenoskenea pellucida* and *Hyalogyrina depressa*.

The entire mantle roof includes large blood sinuses, which are separated from each other by fine fibers of muscle or collagen. The mantle cavity itself is quite large and shows (from left to right) the following structures (Figs. 14a,b; 15a). On the very left, the osphradium forms a round, elevated structure underlain by the osphradial ganglion. Whereas distinct hypobranchial and pallial glands are lacking, the anterior part of the mantle roof is glandular. The single, prominent, bipectinate gill has 19 dorsal and 16 ventral alternating leaflets, which lack a skeleton but are densely ciliated except for flat, interspersed non-ciliated cells, which dominate the distalmost parts of the leaflets (Fig. 15b,c). The gill reaches from the left posterior portion of the mantle roof to the posterior mediodorsal region. Afferent and efferent sinuses are well visible in the sections. At the very left pallial roof the single large, elongated kidney is situated behind the gill, followed by the pericardium with the heart. The right pallial roof is occupied by several loops of the rectum. To the very right there are the openings of the receptaculum and the gonoduct.

Excretory organ, heart and circulatory system

The efferent gill sinus runs backwards and becomes the afferent sinus of the kidney, the ventral (pallial) wall of the latter shows many blood sinuses. The narrow nephropore lies adjacent to the posterior edge of the gill. Whereas the main portion of the kidney shows the typical epithelium with small, round concrements, which are also present in the lumen, the right posterior part of the kidney is glandular (Fig. 15d,e). Posteriorly a ciliated renopericardial duct connects the kidney with the pericardium. Leaving the kidney posteriorly the sinus enters the auricle and ventricle of the monotocardian heart, which is situated behind the kidney. Again the head aorta runs forwards along the median mantle floor.

Genital system (Fig. 16)

Hyalogyrina grasslei is a simultaneous hermaphrodite. The tubular hermaphroditic gonad is composed by two main branches, an anterior and a posterior one, which split into a fan-like structure (Fig. 16a). Spermiogenesis takes place in the outer parts, oogenesis in the inner parts of the tubes (Fig. 16c); both types of germ cells show all stages of development. The fused portion of the two main branches becomes the hermaphroditic duct, which is not glandular but densely filled with sperm for a length of about 250 μm, and is meandering later on. Connected with the latter portion of the hermaphroditic gland there is a prominent blind sac (Fig. 16a,c: bs1), which runs backwards for about 200 μm.

The hermaphroditic duct opens into the glandular part of the gonoduct; it can be divided in several portions on account of distinct mucous cell types. Along the most proximal portion the glandular cells are cuboidal and contain granules which stain heavily. At the line of the posterior end of the mantle cavity the (still closed) lumen of

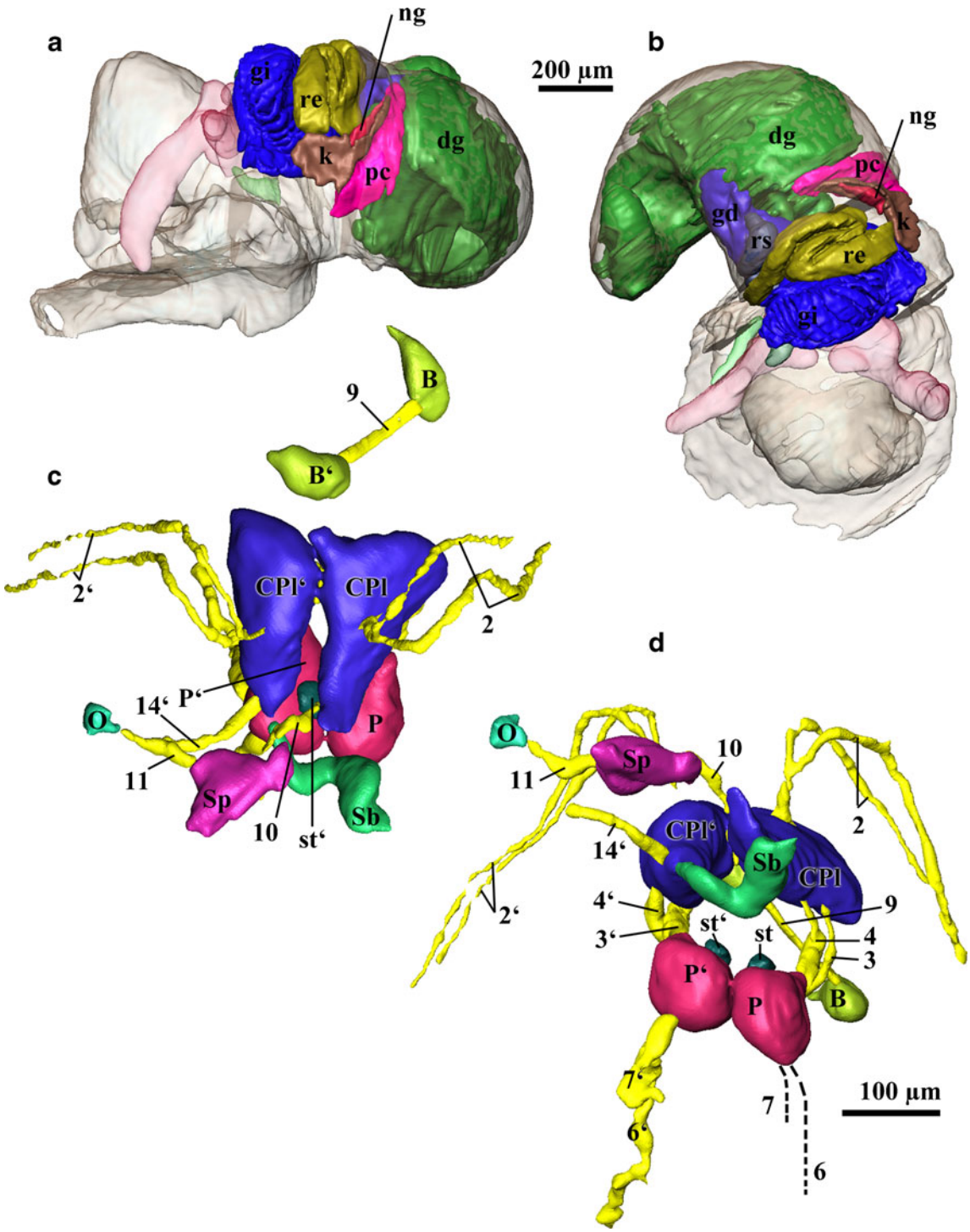

Fig. 14 *Hyalogyrina grasslei*. **a**, **b** Reconstruction of gross anatomy, body wall shown transparent; (**a**) left side view, cephalic tentacles and ciliary knobs in pink; (**b**) anterio-dorsal view. **c**, **d** Reconstruction of nervous system; (**c**) dorsal view, (**d**) posterior view. Labels: B/B' = right/left buccal ganglion, CPl/CPl' = right/left cerebropleural ganglion, dg = digestive gland, gd = gonoduct, gi = gill, k = kidney, ng = nephridial gland, O = osphradial ganglion, P/P' = right/left pedal ganglion, pc = pericardium, re = rectum, rs = receptaculum seminis; Sb = suboesophageal ganglion, Sp = supraoesophageal ganglion, st/st' = right/left statocyst; 2/2' = right/left tentacle nerves, 3/3' = right/left pleuropedal connective, 4/4' = right/left cerebropedal connective, 6/6' = right/left anterior pedal nerve, 7/7' = right/left ventral pedal nerve, 9 = buccal commissure, 10 = supraoesophageal connective, 11 = supraoesophageal-osphradial connective, 14' = left mantle nerve. Supplementary plate 3 offers an interactive 3D model of *Hyalogyrina grasslei* that can be accessed by clicking into Fig. 14 (Adobe Reader version 7 or higher required). Rotate model: drag with left mouse button pressed; shift model: same action+ctrl; zoom: use mouse wheel (or change default action for left mouse button). Select or deselect (or change transparency of) components in the model tree, switch between prefab views, or change surface visualization (e.g. lighting, render mode, crop, etc.)

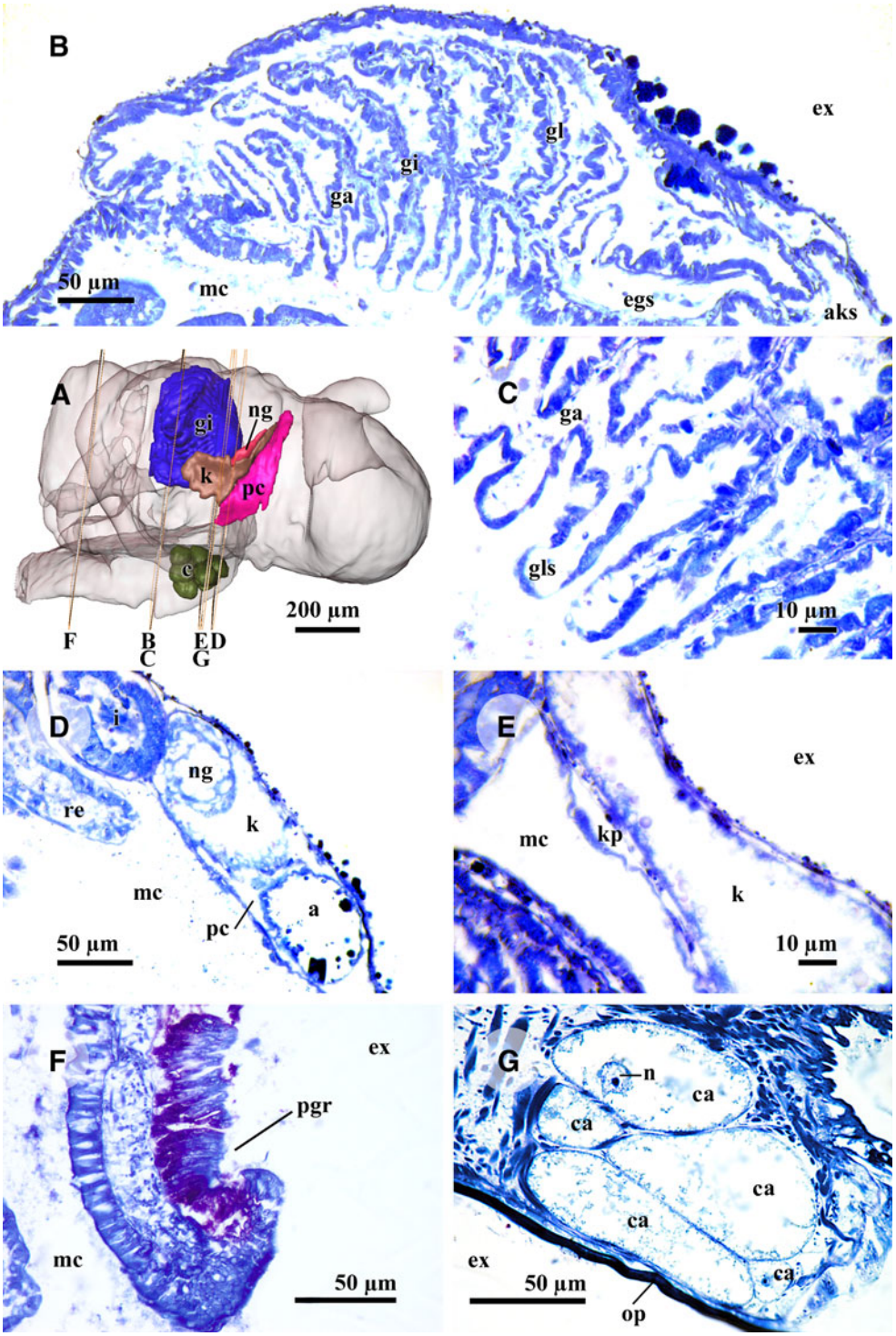

Fig. 15 *Hyalogyrina grasslei*, mantle cavity, histology of gill and other organs. (**a**) Reconstruction of mantle organs in dorsal view, showing section planes. (**b**) Longitudinal section of gill. (**c**) Detail of gill lamellae. (**d**) Overview of kidney and adjacent organs. (**e**) Detail of kidney with papilla. (**f**) Detail of left mantle margin with periostracal groove. (**g**) Metapodium with calcium cells and operculum. Labels: a = heart auricle, aks = afferent kidney sinus, ca = calcium cell, egs = efferent gill sinus, ex = external milieu, ga = gill axis, gi = gill, gl = gill lamellae, gls = sinus of gill lamellae, i = intestine, k = kidney, kp = papilla of kidney, mc = mantle cavity, n = nucleus of calcium cell, ng = nephridial gland, op = operculum, pc = pericardium, pgr = periostracal groove, re = rectum

the gonoduct splits into a ciliated seminal portion (vas efferens) and a thick, glandular oviduct. Both ducts remain associated, however (Fig. 16f). There is a second, narrow, ciliated blind sac (Fig. 16g: bs2) again leading backwards, but this also has a very narrow connection to the distal part of the vas deferens. The thick oviduct shows several prominent mucous cells. The distalmost part of the gonoduct still shows the oviduct and the vas deferens in close association, but there are separate openings for sperm and eggs.

Anterior to the female opening there is the opening of a prominent receptaculum seminis, which runs backwards adjacent to the oviduct nearly to the line of the second blind sac. Its epithelium is densely ciliated (Fig. 16b,d) and underlain by a muscular layer, the lumen is filled with sperm (Fig. 16d,h).

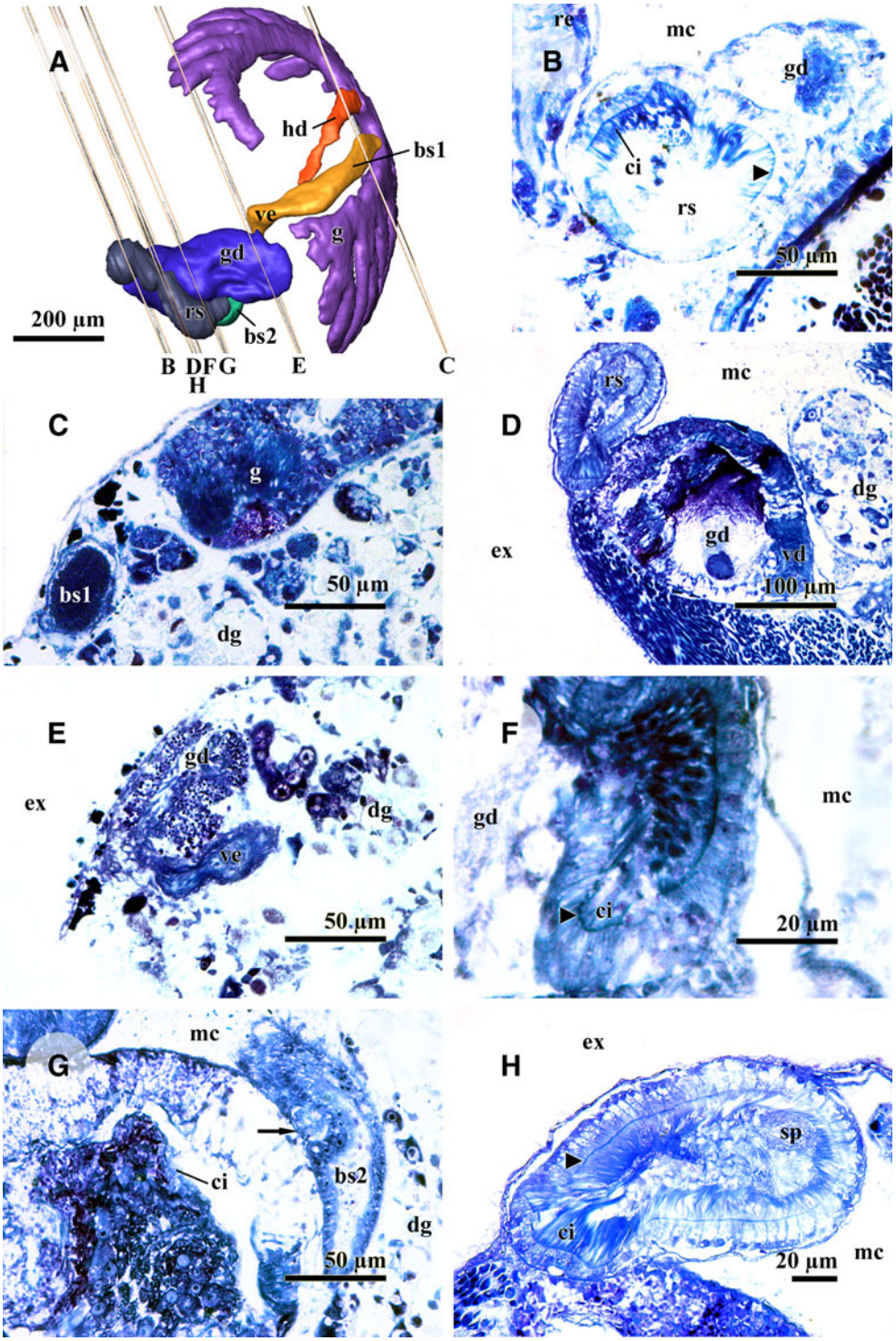

Fig. 16 *Hyalogyrina grasslei*, genital system. **a** Reconstruction of anatomy, showing section planes. **b**–**h** Histological details (arrowhead always marks line of basal bodies of ciliated cells); (**b**) distal end of receptaculum seminis and gonoduct, (**c**) detail of blind sac 1 and adjacent hermaphroditic gonad, (**d**) median part of receptaculum seminis and gonoduct, (**e**) proximal part of gonoduct with vas deferens, (**f**) detail of seminal groove, (**g**) detail of gonoduct and blind sac 2 with connecting duct (*arrow*), (**h**) detail of median part of receptaculum seminis. Labels: bs1/2 = blind sac 1/2, ci = cilia, dg = digestive gland, ex = external milieu, g = gonad, gd = gonoduct, hd = hermaphroditic duct, mc = mantle cavity, re = rectum, rs = receptaculum seminis, sp = autosperm, vd = vas deferens, ve = vas efferens

As outlined above, there is no seminal groove and only a small copulatory organ at the basis of the right cephalic tentacle.

Alimentary tract (Fig. 17)

The whole buccal apparatus is structured nearly identically to that in *Xenoskenea pellucida* and *Hyalogyrina depressa* (see above). Here we recognized a specific paired retractor muscle from the anterior lateral buccal wall to the posterior wall of the head, with an enclosed nerve that originates from the buccal ganglion.

The conditions of the oesophagus and stomach also strongly resemble those in *Xenoskenea*. We recognized five teeth of the gastric shield (Fig. 17f), and the two digestive glands have a common opening into the stomach. The very short intestine starts at the anterior wall of the stomach. The

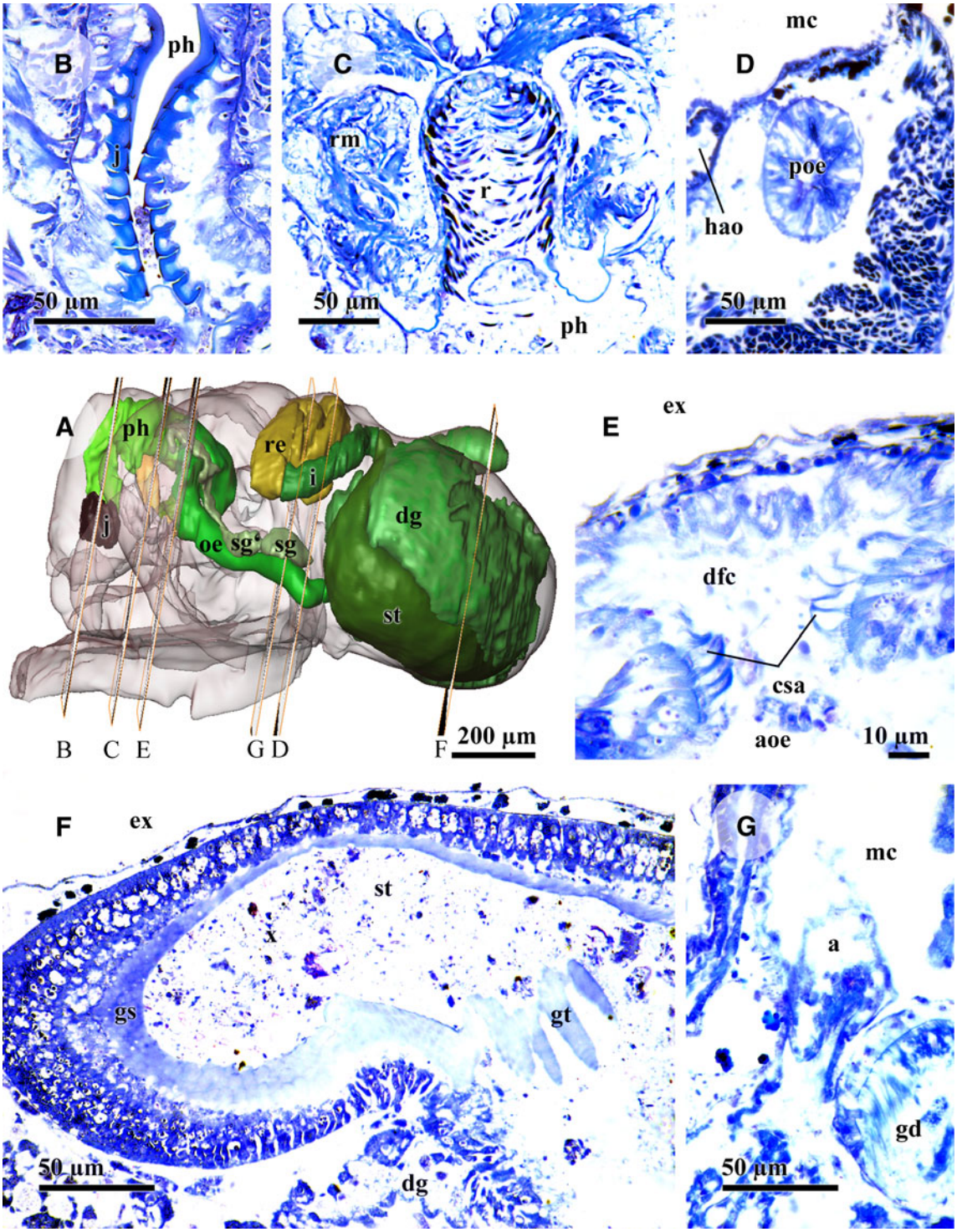

Fig. 17 *Hyalogyrina grasslei*, alimentary tract. **a** Reconstruction of anatomy, left side view, showing section planes. **b**–**g** Histological details; (**b**) cross section of jaws, (**c**) radula with buccal musculature, (**d**) cross section of posterior oesophagus, (**e**) detail of dorsal foot channel in anterior oesophagus, (**f**) stomach with gastric shield and tooth, (**g**) anal opening. Labels: a = anal opening, aoe = anterior oesophagus, csa = ciliary sorting area of stomach, dfc = dorsal food channel, dg = digestive gland, ex = external milieu, gd = gonoduct, gs = gastric shield, gt = spines of gastric tooth, hao = head aorta, i = intestine, j = jaw, mc = mantle cavity, oe = oesophagus, ph = pharynx, poe = posterior oesophagus, r = radula, re = rectum, rm = radular musculature, sg/sg' = right/left salivary gland, st = stomach, x = degraded food

rectum passes beneath the heart, runs forwards to the left, then makes three loops in the pallial roof. The anal opening (Fig. 17g) is situated in the anterior right mantle cavity close to the male opening and shows a free end of the rectal tube.

Nervous system and sensory organs

The nervous system is nearly identical to those in *Xenoskenea pellucida* and *Hyalogyrina depressa* (see, e.g., Fig. 14c,d).

The cephalic tentacles with their bifid tentacular nerves are densely ciliated, except in the outer lateral portions. Eyes are entirely lacking; the small statocysts again contain single statoliths.

Available data from other sources

Warén and Bouchet (1993) described the shell (op.cit.: figs. 39D–G) as small (max. 2.6 mm), very thin, and colourless, and the smooth protoconch as indistinct with 0.6 to 0.7 whorls (fig. 42E). The operculum is multispiral. The short radula is rhipidoglossate with the formula n − 3 − 1 − 3 − n (op.cit.: SEM figs. 40B, C, E); about 20 marginal teeth are present. Concerning external morphology (SEM figs. 41B–D), the animal has a long, tapered snout; eyes are lacking. Three short, flat tentacle-like structures with ciliated edges are situated between the smooth cephalic tentacles with lateral ciliation. A copulatory organ could not be observed even by SEM; the pallial margin is very thick. The foot is bifurcated anteriorly, whereas the posterior end is truncated; epipodial tentacles are lacking. A prominent, bipectinate gill with about 15 leaflets occupies most of the mantle cavity.

The discrepancy concerning the copulatory organ remains obscure: even the SEM photos provided by Warén and Bouchet (1993) do not show any trace of it, whereas our sections revealed it beyond doubt. Since species identity appears certain (we examined paratype material), the only explanation might be that the specimens examined in the two studies differed in sexual maturity.

Hyalogyrina glabra **Marshall, 1988**

(Figures 18, 19 and 20)

External morphology and pedal structures

Again the snout is tapered and the mouth opening is quite small. The smooth cephalic tentacles are quite long, but a copulatory organ is not present. A long, densely ciliated pallial tentacle emerges from the right anterior mantle edge.

There is a single pedal gland, which opens via a wide pore at the anterior border of the foot. Again a densely packed aggregation of large (diameter 80 μm) and transparent calcium cells is found in the center of the foot. The foot sole is densely ciliated.

Shell muscle, haemocoel, and mantle cavity

Concerning the columellar muscle and the histology of the haemocoel the conditions in *H. glabra* appear similar to the preceding species, but histological analysis has been limited due to poor preservation.

The mantle roof (Fig. 18d) is equipped with a dense net of blood sinuses throughout its area. At the very left of the mantle cavity a small osphradium with an underlying ganglion is present (Fig. 20). It is followed to the right by a (left) pallial gland (not shown in Fig. 18) with many, small mucous cells, and more posteriorly by the kidney and the heart. The central mantle cavity is occupied by the gill, and posterior of the latter by the rectal loops with the anal opening on the anterior right side. The genital apparatus with gonoduct and receptaculum fills the right corner of the mantle cavity, the most anterior portion is covered by a pallial gland on the right (Fig. 18: pg).

The gill is again a bipectinate structure without skeleton or bursicles, but is fixed to the pallial roof only at its left side, otherwise it reaches freely into the cavity.

Excretory organ, heart and circulatory system

Conditions of excretory organ (single, left, pallial), heart (monotocardian), and circulatory system (with median head aorta) are nearly identical to those described for the other species investigated. We could not detect a nephridial gland, but this might be due to insufficient preservation.

Genital system (Fig. 19)

The hermaphroditic gonad fills the most posterior part of the body, is a compact organ and shows spermiogenesis in its outer, oogenesis in its inner portions (Fig. 19d). The gonad reaches forwards up to the line of the posterior end of the mantle cavity and is continued by a hermaphroditic duct and the glandular part of the gonoduct, where the lumen is branched into a vas deferens and an oviduct, although both ducts continue forwards in parallel and intimately associated (Fig. 19c). Whereas the vas deferens is a thin, ciliated tube, the oviduct is a thick, glandular structure with a lumen that appears slit-like in cross-sections. Again there are various mucous cell types resulting three distinct portions of the oviduct, and at midlength of the latter there is a small pouch (bs1). Vas deferens and oviduct each have their own openings into the right mantle cavity.

Close to the two genital openings there are two further openings. Laterally at left there is the opening of the separated, tube-like receptaculum seminis, which is surrounded by a muscular layer and has a densely ciliated epithelium (Fig. 19b). It includes up to two spermatophores, with densely packed sperm in one specimen (Fig. 19e). Distally the second opening forms a small cavity (‘genital atrium’) around male and female openings. From there a long, thin flagellum reaches backwards.

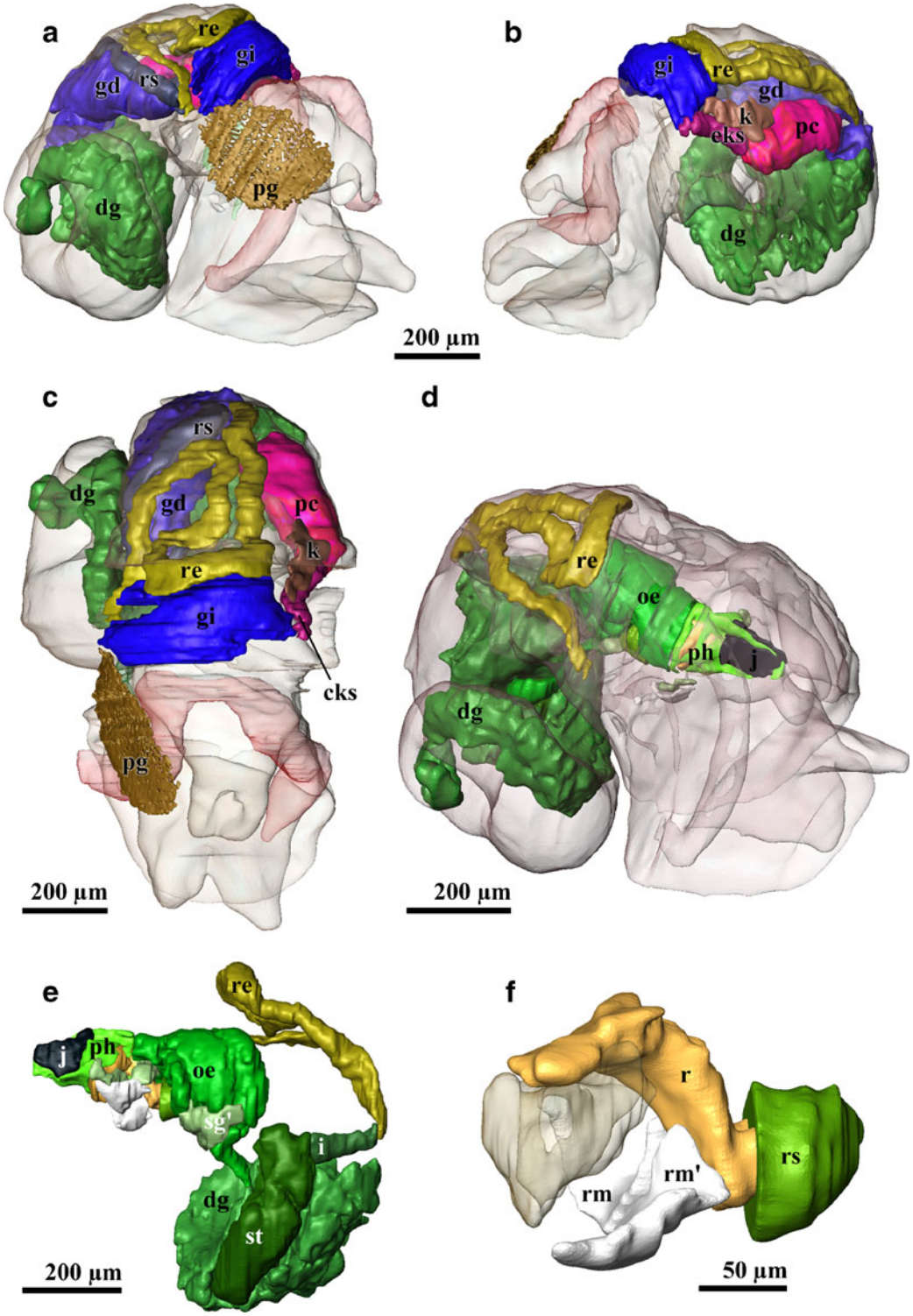

Fig. 18 *Hyalogyrina glabra*. **a**–**c** Reconstruction of mantle organs, body wall shown transparent, mantle roof omitted; (**a**) anterior right-side view, (**b**) left side view, (**c**) dorsal view, anterior is at bottom. **d**–**f** Reconstruction of alimentary tract; (**d**) dorsal right side view, anterior is at right, body wall transparent; (**e**) left side view; (**f**) buccal apparatus in left side view, odontophores transparent. Labels: dg = digestive gland, eks = efferent kidney sinus, gd = gonoduct, gi = gill, i = intestine, j = jaw, k = kidney, oe = oesophagus, pc = pericardium, pg = right side pallial gland, ph = pharynx, r = radula, re = rectum, rm/rm' = right/left radular musculature, rs = radular sheath, st = stomach. Supplementary plate 4 offers an interactive 3D model of *Hyalogyrina glabra* that can be accessed by clicking into Fig. 18 (Adobe Reader version 7 or higher required). Rotate model: drag with left mouse button pressed; shift model: same action+ctrl; zoom: use mouse wheel (or change default action for left mouse button). Select or deselect (or change transparency of) components in the model tree, switch between prefab views, or change surface visualization (e.g. lighting, render mode, crop, etc.)

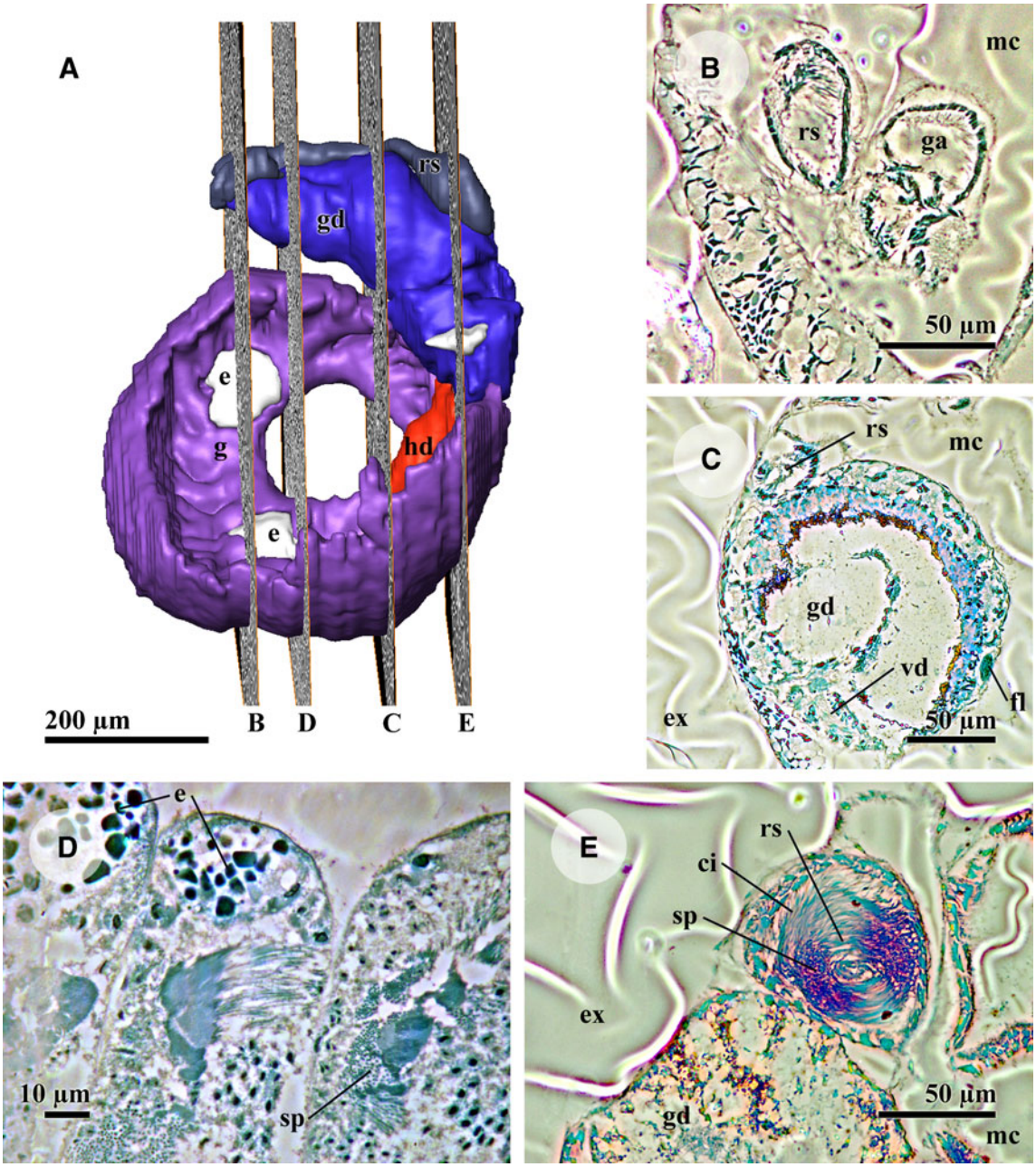

Fig. 19 *Hyalogyrina glabra*, genital system. **a** Reconstruction of anatomy from left side (anterior is at top), showing section planes. **b–e** Histological details, phase contrast microscopy; (**b**) distal end of gonoduct, genital atrium, and receptaculum; (**c**) median portion of gonoduct, duct to receptaculum seminis, and flagellum; (**d**) detail of ovotestis; (**e**) proximal receptaculum seminis with spermatophore. Labels: ci = cilia, e = eggs, ex = external milieu, fl = flagellum, g = gonad, ovotestis, ga = genital atrium, gd = gonoduct, hd = hermaphroditic duct, mc = mantle cavity, rs = receptaculum seminis, sp = autosperm, vd = vas deferens

Unfortunately, the flagellum in the specimen investigated ends at a break, thus could not be analyzed fully.

Alimentary tract (Fig. 18d–f)

The whole buccal apparatus is structured nearly identically to those of the preceding species. Again we recognized a specific paired retractor muscle from the anterior lateral buccal wall to the posterior wall of the head, with an enclosed nerve which contacts the buccal ganglion.

Also the conditions of the oesophagus and stomach strongly resemble those in the other species. We recognized a single tooth of the gastric shield, and the two digestive glands have a common opening into the stomach. The very short intestine starts at the anterior wall of the stomach. The rectum passes beneath the heart, runs forwards to the left, then makes an anterior and a posterior loop in the pallial

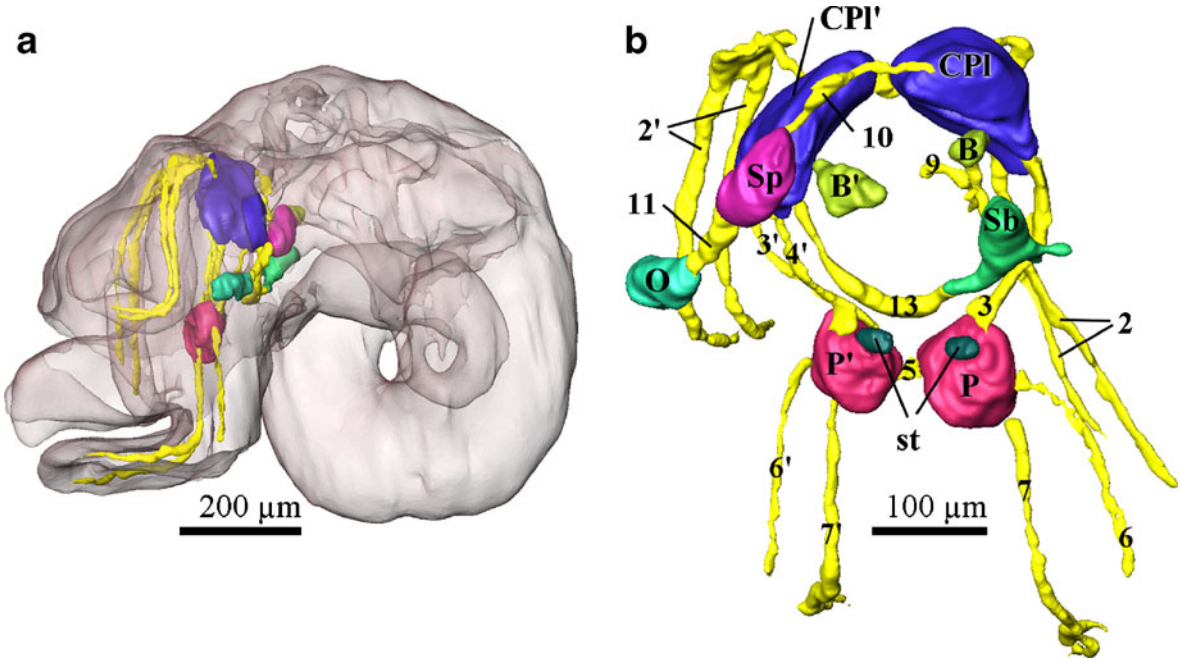

Fig. 20 *Hyalogyrina glabra*, reconstruction of anatomy of nervous system. (**a**) Left side view, body wall shown transparent. (**b**) Dorsal view. Labels: B/B' = right/left buccal ganglion, CPl/CPl' = right/left cerebropleural ganglion, O = osphradial ganglion, P/P' = right/left pedal ganglion, Sb = suboesophageal ganglion, Sp = supraoesophageal ganglion, st = statocysts; 2/2' = right/left tentacle nerves, 3/3' = right/left cerebropedal connective, 4' = left pleuropedal connective, 5 = pedal commissure, 6/6' = right/left anterior pedal nerve, 7/7' = right/left ventral pedal nerve, 9 = buccal commissure (not fully reconstructed), 10 = supraoesophageal connective, 11 = supraoesophageal-osphradial connective, 13 = suboesophageal connective

roof, and finally reaches the anal opening in the anterior right mantle cavity.

Nervous system and sensory organs (Fig. 20)

The epiathroid and streptoneurous nervous system is nearly identical to those in the species described above. Due to insufficient preservation we could not clarify the condition of the posterior visceral loop.

Sensory structures resemble *Hyalogyrina grasslei* in that the cephalic tentacles are supplied by a bifid nerve and eyes are entirely lacking. Again the small statocysts contain single statoliths.

Available data from other sources

Marshall (1988) described the shell as small (max. 1.7 mm), turbinate, transparent, and sculptured (op.cit.: figs. 7F–H, J). The hyperstrophic protoconch has 1.25 whorls (fig. 7I). The radula is rhipidoglossate with the formula n – 1 – 1 – 1 – n, (figs. 16A–D), "the single pair of positionally laterals would seem to be marginals, the original laterals … have presumably been lost" (op.cit.: p. 1000). Marshall also provided a drawing of the head (op. cit.: fig. 9G), which carries a long snout, no eyes, but a filiform 'copulatory organ' (according to our results the pallial tentacle) behind the basis of the right cephalic tentacle. The foot shows two anterior lappets; epipodial tentacles again are lacking.

Hedegaard (1990: pl. 52, fig. 3) figured a shell break demonstrating the shell's purely aragonite structure. Finally Warén and Bouchet (1993: fig. 42D) have provided SEM images of the protoconch that clearly show the hyperstrophic condition.

Hyalogyra expansa Marshall, 1988

Anatomy and histology

Because of the very poor preservation of the specimens available, only a superficial description can be provided which focuses on differences to the species described above.

There is only a single pedal gland, which is quite large and lies in the anterior foot.

The single (left) ctenidium is quite large, bipectinate, and lacks skeletal support. Its anterior half reaches free into the mantle cavity. Again there is a monotocardian heart and a single (left) kidney lying in the pallial roof. The single (left) hypobranchial gland shows three distinct regions differing in histology. In addition, a huge medio-dorsally placed pallial gland (brood pouch?) with various cell types is present. More posteriorly a separated, glandular (much narrower), tubular vas deferens (prostate gland) opens into the mantle cavity.

This species represents another simultaneous hermaphrodite, and again the genital apparatus as a whole is a very complex system. The hermaphroditic gland shows distinct regions of sperm (outwards) and egg (inwards) production. The eggs are very large (more than 200 μm in diameter) and yolk-rich. There is a receptaculum below and posterior to the heart on the left side; a ciliated duct connects the receptaculum to the mantle cavity. A copulatory organ is situated behind the right cephalic tentacle and is supplied by a nerve from the cerebropleural connnective. The posterior basis of the copulatory organ is provided with another short appendix.

The entire buccal apparatus resembles those in the *Hyalogyrina* species, but each buccal retractor clearly shows a nerve inside. The anterior oesophagus has two main dorsal folds and shows torsion, and there are true, separate oesophageal glands (not pouches). The posterior oesophagus is not folded. The stomach is again equipped with gastric shield and ciliary fields. Intestinal loops are found only below the posterior mantle cavity; there is no anterior loop. The very thick pallial gonoduct shifts the pallial rectum far to the left side of the mantle cavity.

The nervous system is again epiathroid and streptoneurous and strongly resembles those in the *Hyalogyrina* species. A so-called juxtaganglionar organ (e.g. Clare 1987; Herbert 1982; Martoja 1965a, b; Switzer-Dunlap 1987) lies at the dorsal side of the short cerebral commissure. The statocysts are attached at the posterior-ventral side of the pedal ganglia and again contain a single statolith each.

Available data from other sources

Marshall (1988) described the shell as small (max. 2.65 mm), depressed to flat, thin, and transparent (op.cit.: fig. 7A–C, E), the orthostrophic protoconch as with 1.2 whorls (fig. 7D). The radula is rhipidoglossate with the formula n – 6 – 1 – 6 – n (fig. 15D–G). According to Marshall's drawing of the head (op.cit.: fig. 9F), the latter shows a depressed snout, no eyes, flattened cephalic tentacles, and behind the right tentacle one another slender one (copulatory organ). The anterior foot is deeply bifurcated and lacks epipodial tentacles.

Discussion

For direct anatomical comparisons among the basal heterobranch families we use the following references.

Ectobranchia (Valvatoidea):

Cornirostridae: Ponder (1990b, 1991a), Bieler et al. (1998);
Xylodisculidae: Warén (1992), Høisaeter and Johannessen (2002);
Valvatidae: Bernard (1890), Yonge (1947), Starmühlner (1952), Cleland (1954), Johansson (1956), Sitnikova (1984), Rath (1986, 1988), Falniowski (1989, 1990);
Orbitestellidae: Ponder (1990a, 1991a);

Architectonicoidea:

Architectonicidae: (Haszprunar 1985b);
Mathildidae: (Haszprunar 1985c);
Omalogyridae: Fretter (1948), Bäumler et al. (2008);

Rissoelloidea:

Rissoellidae: Fretter (1948), Simone (1995), Wise (1998).

Character analysis

Hyperstrophic protoconch

The functional significance of hyperstrophic larval shells (protoconch II), i.e. those with the direction of coiling opposite to the anatomical asymmetry (cf. Robertson 1993), still is an enigma despite the generally accepted systematic value of the feature. Indeed, this was the decisive character for Warén and Bouchet (1993) to transfer the genus *Hyalogyrina*—previously considered as a skeneid vetigastropod (Marshall 1988; Rubio et al. 1992)—to the Heterobranchia. Hadfield and Strathmann (1990) claimed that also certain trochoidean species should have hyperstrophic protoconchs. However, as outlined by Warén and Bouchet (1993), Vetigastropoda never have a true larval shell (protoconch II; see, e.g., Bandel 1982), as their protoconch solely consists of an embryonic shell (i.e. protoconch I) without any true coiling, although deformations can occur. Accordingly, the term 'hyperstrophy' should not be applied to an embryonic shell; thus, 'heterostrophy' (i.e. the different orientation of coiling in larval and adult shells; cf. Robertson 1993) is principally restricted to taxa with larval shells, namely the Neritimorpha, Caenogastropoda, and Heterobranchia. Despite certain exceptions (e.g. the Rissoellidae), heterostrophy remains one of the major diagnostic characters of marine Heterobranchia. In the Hyalogyrinidae heterostrophy is generally weakly developed due to their lecithotrophic mode of development (see below). A hyperstrophic protoconch can be visible by SEM in *Hyalogyrina* species, but seems to be indistinctly developed in *Xenoskenea* and *Hyalogyra*.

External morphology

Nearly all ectobranch species have a very typical external appearance mainly characterized by a bifid anterior foot, a tapered (sometimes also bifid) snout, one or two pallial tentacles at the right mantle edge, and a gill that can be extended out of the mantle cavity (for images of live

ectobranchs see, e.g., Fechter and Falkner 1990; Høisaeter and Johannessen 2002; Ponder 1990b, 1991a; Warén et al. 1993). Whereas foot and snout characteristics are common among the lower Heterobranchia, the latter characters appear to be diagnostic for Ectobranchia. Warén et al. (1993) did not describe a gill for *Xylodiscula boucheti* and *X. lens*, but Høisaeter and Johannessen (2002) figured a typical ectobranch gill for *X. planata.* In the Orbitestellidae a gill is entirely lacking in the few species in which the soft parts have been studied. Since valvatids of similar size (i.e. about 1 mm; e.g. *Valvata cristata, V. relicta*) do have a gill, it is unlikely that the lack of a gill is due to small size. Instead, this difference suggests a more distant relationship, as is also indicated by molecular characters (Dinapoli and Klussmann-Kolb 2010; Jörger et al. 2010). The pallial tentacle is densely ciliated and generates a strong exhalant current for mantle sanitation, as reported for Cornirostridae and Valvatidae.

Pedal characters

Most Caenogastropoda (except, e.g., the cerithioid Litiopidae and certain Bittiniinae; Ponder 1991b) and all Heterobranchia are devoid of epipodial tentacles, such as occur in all Hyalogyrinidae and Ectobranchia. The posterior foot tentacle in *Xenoskenea pellucida* and the still undesribed *Xenoskenea* species from Japan (Fig. 1) might be used for generic diagnosis.

A second pedal gland, present in *Xenoskenea* in the center of the foot mass, also occurs in Orbitestellidae, but not in the other ectobranch families. This character has also been described in other allogastropod taxa, namely in the Architectonicidae, Mathildidae, and Omalogyridae.

The mass of 'calcium cells' in the posterior foot appears as a diagnostic synapomorphy of the Hyalogyrinidae. Calcium cells are a specialized type of rhogocytes (also termed pore cells; cf. Haszprunar 1996; Sminia and Boer 1973). Since we did not determine the metal ion of the cell content, we cannot exclude the possibility that these cells are involved in ion metabolism of elements other than calcium, although the typical (e.g. Sminia et al. 1976) transparent appearance favors the latter assumption.

Mantle cavity

The general conditions and structures of the hyalogyrinid mantle cavity strongly resemble those in Valvatidae, Cornirostridae, and probably also Xylodisculidae. The most prominent organ is the bipectinate gill, which can be extended out of the mantle cavity, a condition diagnostic for Ectobranchia. As already outlined by Rath (1986, 1988), Haszprunar (1985a, 1988), and Ponder and Lindberg (1997), the ectobranch gill differs from true ctenidia in variability, structure (no skeleton, entirely ciliated) and mode of development, and is regarded as a secondary structure. As in Valvatidae (see review by Rath 1988), the gill morphology and in particular the mode of fixation at the mantle roof differs significantly between the hyalogyrinid species.

On the whole, the arrangement of pallial organs, particularly the presence of large pallial glands and the kidney, is typical for basal Heterobranchia. However, due to the prominent gill and the ciliated pallial tentacle there are no ciliary strips for ventilation as are otherwise found in these taxa (Haszprunar 1985a, b, c, 1988; Robertson 1985), e.g. in Orbitestellidae, Omalogyridae, Architectonicoidea, Acteonoidea, and Pyramidelloidea (according to Jörger et al. 2010, the latter group appears as more closely related to pulmonate taxa).

Heart, circulatory and excretory system

The monotocardian heart, a single (left) kidney lying in the pallial roof, and in particular the type of circulatory system (mantle roof/gill –> kidney –> heart –> aorta at median mantle bottom) are all conditions typical of basal Heterobranchia (Haszprunar 1985a, b, c, 1988; Ponder and Lindberg 1997).

Genital apparatus

A thorough discussion on the evolution of the genital systems is hindered by several facts. (A) Conditions differ significantly between species and families, and the taxon sampling of Ectobranchia is still quite poor (less than 10%); the Xylodisculidae have not been studied anatomically. (B) In most cases only a few preserved specimens have been available. (C) Because ectobranchs (basal Heterobranchia in general) are simultaneous hermaphrodites with internal fertilization, genital conditions are always very complicated, so that poorly preserved specimens make only minimal contributions to our understanding.

Healy (1993) described the fine structure of the sperm of *Xenoskenea pellucida* and of an unnamed "*Hyalogyrina*" species from hydrothermal vents off Fiji (no further data on the specimen studied were provided, it may be conspecific with *Xylodiscula major* Warén & Bouchet, 1993 from the same locality). Healy outlined the great spermatological similarities among all families of Ectobranchia, their general heterobranch affinities, and their distinctness from other heterobranch taxa.

Whereas a prominent copulatory organ is present in Cornirostridae, Orbitestellidae and Valvatidae, the same is not the case in Xylodisculidae (data available only for *Xylodiscula vitrea, X. eximina,* and *X. planata*) and Hyalogyrinidae. These conditions vary significantly among the basal heterobranch taxa: some (e.g. Architectonicidae, Mathildidae, Omalogyridae) provide fertilization solely by spermatophores and entirely lack a copulatory organ; others

(e.g. Rissoellidae) do have a penis. Accordingly, it is likely that copulatory organs have evolved independently within the Ectobranchia. In *Xenoskenea pellucida* the very small copulatory organ may function in combination with the prominent mantle lappet during copulation.

It remains unclear where and how fertilization takes place in the Hyalogyrinidae. The various glands in the male gonoduct and the lack of a prominent copulatory organ suggest spermatophore production. Indeed, we found spermatophores in the gonoducts of *Xenoskenea pellucida* and *Hyalogyrina glabra*. A prominent receptaculum is generally present, its opening is entirely separated from those of the remaining gonoducts. Such genital conditions resemble those in Architectonicidae and Mathildidae, thus might be plesiomorphic for Ectobranchia and Heterobranchia in general. Since most heterobranchs have large gelatinous egg masses, which are obviously produced after fertilization within the gonoduct, fertilization probably takes place proximally. In addition, the heterobranch sperm is a typical introsperm (Jamieson 1987), which again suggests fertilization within the genital system. Finally, the valvatid *Borysthenia naticina* (Menke, 1845) is known to be ovoviviparous (Velitchkowsky in Lindholm 1927), which requires internal fertilization.

Due to differences in preservation and staining methods as well as among investigators, and because of the high complexity in general, homologization of the various glandular portions of the genital system is risky. We provide a comparative scheme of gonoducts (Fig. 21), but want to stress that the various terms applied to each species are somewhat speculative (Fig. 22).

Judging from protoconch morphology (i.e. short and smooth larval shell) and egg histology (yolk-rich as far as available), it is likely that ectobranchs generally have a lecithotrophic or intracapsular mode of development. Spawn is known only from *Cornirostra pellucida* (Ponder 1990b) and from Valvatidae (e.g. Kruglow and Frolenkova 1981; Rath 1986): Whereas the latter show egg-connecting strings, so-called chalazae, which are typical for Heterobranchia, this is not the case in *Cornirostra*. On the other hand, *Cornirostra* produces a gelatineous spawn matrix, again a character typical for Heterobranchia, whereas Valvatidae (except *Borysthenia*) have a capsular spawn.

Ontogeny is virtually unknown in all Ectobranchia, except in *Valvata tricarinata*, for which Furrow (1935) reported on the ontogeny of the genital system, and in *Valvata piscinalis*, for which a direct mode of development has been described in detail (Rath 1986).

Alimentary tract

The rhipidoglossate radula of the Hyalogyrinidae is strikingly similar to those in several 'archaeogastropod' taxa (Cocculinida, Neomphalida, Vetigastropoda), thus is considered as homologous and, by outgroup comparison, as plesiomorphic to Ectobranchia and Heterobranchia, respectively. Accordingly, the taenioglossate type found in Valvatidae and other basal Heterobranchia (e.g. Mathildidae) must have evolved independently from those in Caenogastropoda.

Jaws consisting of tooth-like elements are present in Vetigastropoda and Neomphalida, and are also often found among the Heterobranchia, accordingly they are considered as plesiomorphic structures like the rhipidoglossate radula. Also the presence of a dorsal food channel in the buccal roof and the anterior oesophagus is a plesiomorphic feature of Heterobranchia. In contrast, the remaining anterior alimentary tract shows typical (apomorphic) heterobranch conditions: large, tubular salivary glands composed of large cells with extraordinarily large nuclei, replacement of true cartilages by a purely muscular cushion, absent or at most vestigial oesophageal glands. Sasaki (1998) discussed a number of "trends" in the evolution of the buccal mass from Tryblidia to Gastropoda, and from the archaeogastropod to the caenogastropod level of organisation, whereas Heterobranchia were not considered. However, at least one major 'trend', the reduction of buccal muscles, is also observable in Ectobranchia compared with ('skeneimorph') vetigastropods or neomphalidans of similar size range. Of particular interest are the paired buccal protractors with a specific enclosed nerve found in certain hyalogyrinid species (if preservation was sufficient): the same structure is present also in Architectonicidae (see Haszprunar 1985b: fig. 2), Mathildidae and Pyramidellidae (GH pers. obs.). This structure is very delicate and easily overlooked. Since it has also been found in the valvatid *Borysthenia naticina* (GH pers. obs.), this character likely constitutes another synapomorphy of Heterobranchia and, thus, a plesiomorphy for Ectobranchia.

Whereas the conditions of the stomach with gastric shield and tooth, ciliary fields, and paired digestive glands reflect gastropod plesiomorphies, the very short intestine is unusual for detritovorous gastropods, but again typical for Ectobranchia and basal heterobranchs in general. Parallel to, e.g., seguenzoid (GH pers. obs., e.g. on *Carenzia carinata*) and certain 'skeneimorph' Vetigastropoda (e.g. Kunze and Haszprunar 2008) or to certain hydrobiid Caenogastropoda, the pallial portion of the rectum makes two to three loops occupying a considerable portion of the pallial roof.

Nervous system and sensory organs

Epiathroid and streptoneurous conditions of the nervous system are typical for sorbeoconch Caenogastropda and basal Heterobranchia, and exclude the Hyalogyrinidae from Vetigastropoda, Neomphalida or architaenioglossate Caenogastropoda, since these latter taxa show hypoathroid

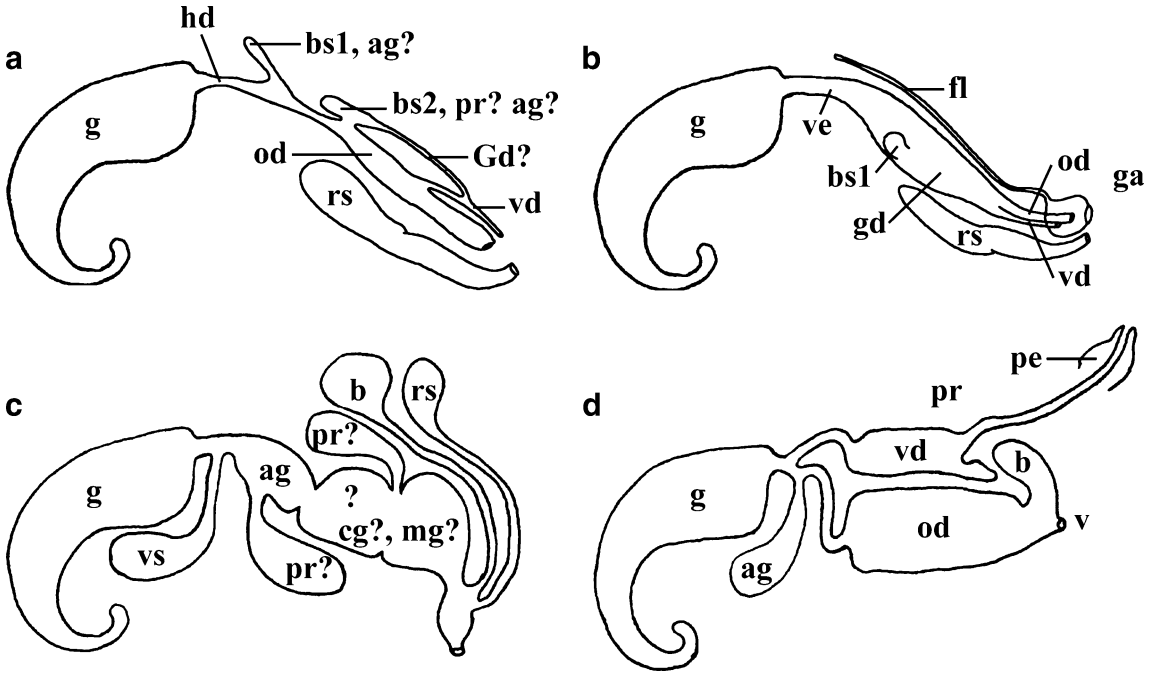

Fig. 21 Schematic comparison of the genital systems of hyalogyrinid species. (**a**) *Hyalogyrina grasslei*. (**b**) *Hyalogyrina glabra*. (**c**) *Hyalogyrina depressa*. (**d**) *Xenoskenea pellucida*. Labels: ag = albumen gland, b = bursa, bs1/2 = blind sac 1/2, cg = capsule gland, fl = flagellum, g = hermaphroditic gonad, ga = genital atrium, Gd = Garnault's duct (as described for *Valvata piscinalis* by Garnault 1890), gd = gonoduct, hd = hermaphroditic duct, mg = mucous gland, od = oviduct, pe = penis, pr = prostate gland, rs = receptaculum seminis, v = vaginal opening, vd = vas deferens, ve = vas efferens, vs = ventral sac

conditions. As in Architectonicidae and Mathildidae, the tentacular nerve in Ectobranchia is bifid.

The juxta-ganglionar organ has been reported from gastropods only occasionally (e.g. Clare 1987; Herbert 1982; Martoja 1965a, b; Switzer-Dunlap 1987), but is probably present in all species. It has been identified tentatively as a neuro-endocrine organ involved in reproductive biology (Switzer-Dunlap 1987) and potentially homologous with the paired "dorsal bodies of pulmonates" (Luchtel et al. 1997).

The smooth and densely ciliated cephalic tentacles and the lack of epipodial structures are both typical for basal Heterobranchia. Among the hyalogyrinids studied so far, eyes are present only in the shallow-water *Xenoskenea pellucida*; these are closed vesicles and equipped with a sphaerical lens. The two types of statocyst content, single statoliths or several statoconia, are scattered throughout the gastropod system, but constant within major groups: whereas Ectobranchia generally show the statolith type, statoconia are present, e.g., in Architectonicoidea.

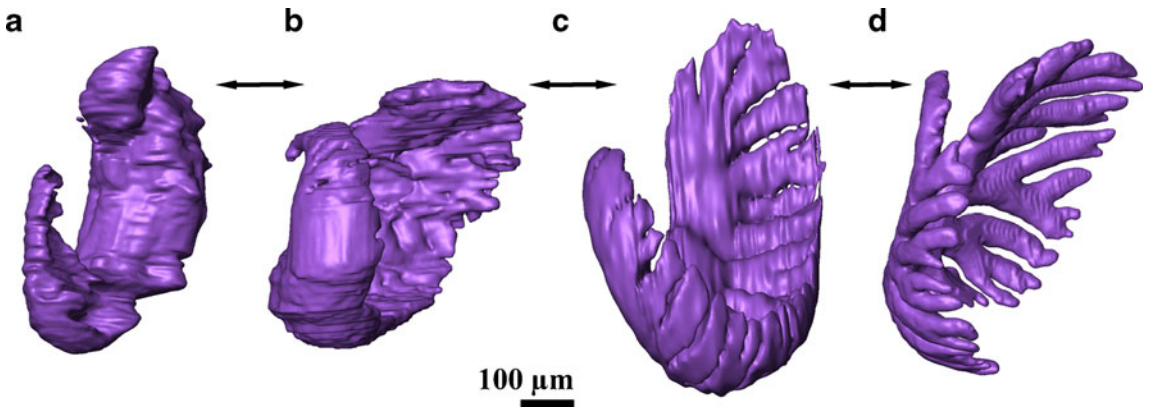

Fig. 22 Series of hermaphroditic glands in Hyalogyrinidae; anterior views, differences in lobation do not correlate with size. (**a**) *Xenoskenea pellucida*. (**b**) *Hyalogyrina glabra*. (**c**) *Hyalogyrina depressa*. (**d**) *Hyalogyrina grasslei*

Affinities of Hyalogyrinidae

Generic division of Hyalogyrinidae

Marshall (1988) noted the close affinity of *Hyalogyrina* with *Hyalogyra* and distinguished the two genera mainly on radula characters: *Hyalogyra expansa* (formula n − 6 − 1 − 6 − n) has considerably more lateral and marginal teeth than *Hyalogyrina* (formula n − 1 − 1 − 1 − n). *Xenoskenea pellucida* has a third kind of radula (n-3-1-3-n according to Warén et al. 1993) and is also clearly different from both other genera in showing eyes, distal appendages of the snout, the single tentacle at the posterior end of the foot, the large mantle pad, and a small but true copulatory organ. Accordingly, *Hyalogyra* and *Hyaloyrina* appear more closely related to each other than to *Xenoskenea.*

Position of Hyalogyrinidae among the Ectobranchia and Heterobranchia

We regard Linnean ranks solely as expressions of a relative hierarchy, thus we do not argue pro or contra superfamilial (Valvatoidea) versus higher rank (Ectobranchia). Ectobranchia is preferred, because (1) Valvatoidea (often cited as Valvatida or Valvatacea) is also a major group of sea-stars, and (2) Ectobranchia is independent of ranking and refers to a clear synapomorphy of the group, the ectobranch gill condition (the inclusion of the gill-less Orbitestellidae cannot be substantiated by any morphological character and is contradicted by the molecular analyses; Dinapoli and Klussmann-Kolb 2010). Among the Heterobranchia (see below), Ectobranchia (Valvatoidea) are clearly characterized by plesiomorphic and apomorphic characters:

Plesiomorphic traits mainly concern the alimentary tract, where paired jaws composed of teeth and a dorsal food channel in the buccal roof and the anterior oesophagus are still present and the stomach is still equipped with a cuticularized gastric shield and tooth as well as with ciliary sorting areas. Concerning the radula there is a clear trend to reduce the number of teeth per row: Hyalogyrinidae still show the rhipidoglossate type; Cornirostridae and Valvatidae have a taenioglossate radula with 7 or 9 teeth per row (see Warén et al. 1993 for discussion); Xylodisculidae (formula 2 − 1 − 0 − 1 − 2) lack a rhachidian tooth; and Orbitestellidae have only three teeth per row (1-1-1). This transformation series of the radula type character places Hyalogyrinidae at the basis of Ectobranchia by outgroup comparison, since a re-establishment of the rhipdioglossate type looks very improbable.

Van den Biggelaar and Haszprunar (1996) showed that *Valvata piscinalis* differentiates its mesentoblast 4d cell at the 40-cell stage, whereas opisthobranch and pulmonate taxa do that at the 24-cell stage already. This acceleration has occurred in parallel in the evolution to architaenioglossate (44- to 48-cell stage) and sorbeoconch (40- to 24-cell stage) Caenogastropoda. Together with the other plesiomorphies of the gut (see above) this suggests Ectobranchia as the most basal extant offshoot among the Heterobranchia.

Ectobranch synapomorphies are particularly the diagnostic gill (for Orbistestellidae see above) and the pallial tentacles used for exhalant water current. In addition, a couple of sperm characters (see Healy 1993 for details) separate Ectobranchia from Architectonicoidea and all other heterobranch groups. Also the recent study of Dinapoli and Klussmann-Kolb (2010) placed *Cornirostra* and *Valvata* (but not *Orbitestella*) in a single clade close to the origin of Heterobrachia. All current data on the Hyalogyrinidae support the concept of monophyly of the Ectobranchia.

The taxon sampling among the ectobranch taxa is still quite poor, and it is likely that several more taxa currently seen as skeneids, vitrinellids or cyclostrematids are in fact ectobranchs. In addition, the Xylodisculidae and several other basal heterobranch taxa (e.g. Tjaernoiidae, Murchisonellidae, Aclididae, Cimidae) remain unstudied. Therefore, an unambiguous phylogenetic analysis of the other families among the Ectobranchia cannot be provided. Nevertheless, Hyalogyrinidae can be reasonably placed at the very basis of Ectobranchia and Heterobrachia, suggesting an origin of Heterobranchia from the rhipidoglossate level of gastropod evolution. However, this does not necessarily mean that the hypothesis of monophyletic Apogastropoda (Caenogastropoda and Heterobranchia) is obsolete: although a synapomorphic taenioglossate condition of the radula is no longer supported, in particular sperm characters (Healy 1993; Ponder and Lindberg 1997) still suggest a common origin of Caenogastropoda and Heterobranchia; the rhipidoglossate sister group for both remains unresolved at the present stage of knowledge. Thus, the story will continue: anatomical, spermatological and molecular studies on more basal heterobranch taxa are needed to provide a robust phylogenetic framework of the origin and early evolution of the Heterobranchia.

Acknowledgements We are very grateful to all colleagues who added material and data to the present study: the specimens of *Xenoskenea pellucida* were collected by Dr. Serge Gofas (Universidad de Malaga, Spain) during “Mission Algarve”, a workshop in southern Portugal organised by Dr. Philippe Bouchet (Museum National d’Histoire Naturelle, Paris). Bruce A. Marshall (Museum of New Zealand, Te Papa Tongarewa) kindly provided the specimens of *Hyalogyrina glabra* and *Hyalogyra expansa.* Dr. Kazunori Hasegawa (National Museum of Nature and Science, Tsukuba City, Japan) kindly made specimens of *Hyalogyrina depressa* available to us. Dr. Anders Warén (Naturhistoriska Riksmuseet, Stockholm) sent us material of *Hyalogyrina grasslei*, provided SEM photos of various hyalogyrinids, and added (as did two anonymous referees) much helpful advice to the draft of this paper. We also acknowledge technical support from Ms. Eva Lodde (ZSM) and Heidemarie Gensler (LMU Munich). Last but not least we thank Dr. Masanori Taru (Toho University, Japan) for providing his beautiful live photo of a new *Xenoskenea* species.

References

Aktipis, S. H., Giribet, G., Lindberg, D. R., & Ponder, W. F. (2008). Gastropoda. In W. F. Ponder & D. R. Lindberg (Eds.), *Phylogeny and evolution of the Mollusca* (pp. 199–236). Berkeley: University of California Press.

Bandel, K. (1982). Morphologie und Bildung der frühontogenetischen Gehäuse bei conchiferen Mollusken. *Facies (Erlangen), 7*, 1–198. pls. 1–22.

Bandel, K. (1991). Gastropods from brackish and fresh water of the Jurassic-Cretaceous transition (a systematic reevaluation). *Berliner Geowissenschaftliche Abhandlungen, (A), 134*, 9–55.

Bandel, K. (1996). Some heterostrophic gastropods from Triassic St. Cassian formation with a discussion on the classification of the Allogastropoda. *Paläontologische Zeitschrift, 70*, 325–365.

Bandel, K., & Heidelberger, D. (2002). A Devonian member of the subclass Heterostropha (Gastropoda) with valvatoid shell shape. *Neues Jahrbuch für Geologie und Paläontologie Monatshefte, 2002*(9), 503–550.

Bäumler, N., Haszprunar, G., & Ruthensteiner, B. (2008). 3D interactive microanatomy of *Omalogyra atomus* (Philippi, 1841) (Gastropoda, Heterobranchia, Omalogyridae). In D. Geiger, & B. Ruthensteiner (Eds.) *Micromolluscs: Methodological challenges – exciting results*. *Zoosymposia*, *1*, 108–116.

Bernard, F. (1890). Recherches sur *Valvata piscinalis*. *Bulletin Scientifique de la France et de la Belgique, 22*, 253–361. pls. 12–20.

Bieler, R., Ball, A. D., & Mikkelsen, P. M. (1998). Marine Valvatoidea – Comments on anatomy and systematics with description of a new species from Florida (Heterobranchia: Cornirostridae). *Malacologia, 40*, 305–320.

Clare, A. S. (1987). Studies on the juxtaganglionar organ of trochids. In H. H. Boer, W. P. M. Geraerts, & J. Joosse (Eds.), *Neurobiology: Molluscan models. Proceedings of the 2nd symposium on molluscan neurobiology, Amsterdam 1986* (pp. 342–349). Amsterdam: North Holland Publ. Comp.

Cleland, D. M. (1954). A study of the habits of *Valvata piscinalis* (Müller) and the structure and function of the alimentary canal and reproductive system. *Proceedings of the Malacological Society of London, 30*, 167–203.

Colgan, D. J., Ponder, W. F., Beacham, E., & Macaranas, J. M. (2003). Gastropod phylogeny based on six segments from four genes representing coding or non-coding and mitochondrial or nuclear DNA. *Molluscan Research, 23*, 123–148.

Dayrat, B., & Tillier, S. (2003). Molecular systematics of the major lineages of the Gastropoda. In C. Lydeard & D. R. Lindberg (Eds.), *Molecular systematics and phylogeography of mollusks* (pp. 161–184). Washington & London: Smithsonian Series on Evolutionary Biology. Smithsonian Books.

Dinapoli, A., & Klussmann-Kolb, A. (2010). The long way to diversity – Phylogeny and evolution of the Heterobranchia (Mollusca: Gastropoda). *Molecular Phylogeny and Evolution, 55*, 60–76.

Falniowski, A. (1989). A critical review of some characters widely used in the systematics of higher taxa of freshwater prosobranchs (Gastropoda: Prosobranchia), and a proposal of some new, ultrastructural ones. *Folia Malacologica (Kraków), 3*(1216), 73–94.

Falniowski, A. (1990). Anatomical characters and SEM structure of radula and shell in the species-level taxonomy of freshwater prosobranchs (Mollusca: Gastropoda: Prosobranchia): a comparative usefulness study. *Folia Malacologica (Kraków), 4*(1276), 53–142.

Fechter, R., & Falkner, G. (1990). *Weichtiere. Europäische Meeres- und Binnenmollusken*. München: Mosaik Verlag.

Fischer, P. (1880–1887). *Manuel de conchyliologie et de paléontologie conchyliologique*. Paris: Savy. [Fascicule 7 with pp. 609–688 published 30 June 1884.]

Fretter, V. (1948). The structure and life history of some minute prosobranchs of rock pools: *Skeneopsis planorbis* (Fabricius), *Omalogyra atomus* (Philippi), *Rissoella diapha* (Alder) and *Rissoella opalina* (Jeffreys). *Journal of the Marine Biological Association of the UK, 27*, 597–632.

Furrow, C. L. (1935). Development of the hermaphroditic genital organs of *Valvata*. *Zeitschrift für Zellforschung und Mikroskopische Anatomie, 22*, 282–304.

Garnault, P. (1890). Les organes reproducteurs de la *Valvata piscinalis*. *Bulletin Scientifique de la France et de la Belgique, 22*, 496–507. pl. 26.

Grande, C., Templado, J., & Zardoya, R. (2008). Evolution of gastropod mitochondrial genome arrangements. *BMC Evolutionary Biology, 8*(61), 1–15.

Hadfield, M. G., & Strathmann, M. F. (1990). Heterostrophic shells and pelagic development in trochoideans: implications for classification, phylogeny and palaeoecology. *Journal of Molluscan Studies, 56*, 239–256.

Hartmann, H., Heß, M., & Haszprunar, G. (2011). Interactive 3D anatomy and affinities of Bathysciadiidae (Gastropoda, Cocculinoidea): deep-sea limpets feeding on decaying cephalopod beaks. *Journal of Morphology, 272*, 259–279.

Hasegawa, K. (1997). Sunken wood-associated gastropods from Suruga Bay, Pacific side of the central Honshu, Japan, with description of 12 new species. *National Science Museum Monographs, 12*, 59–123.

Haszprunar, G. (1985a). The Heterobranchia – a new concept of the phylogeny of the higher Gastropoda. *Zeitschrift für Zoologische Systematik und Evolutionsforschung, 23*, 15–37.

Haszprunar, G. (1985b). Zur Anatomie und systematischen Stellung der Architectonicidae (Mollusca, Allogastropoda). *Zoologica Scripta, 14*, 25–43.

Haszprunar, G. (1985c). On the anatomy and systematic position of the Mathildidae (Mollusca, Allogastropoda). *Zoologica Scripta, 14*, 201–213.

Haszprunar, G. (1988). On the origin and evolution of major gastropod groups, with special reference to the Streptoneura. *Journal of Molluscan Studies, 54*, 367–441.

Haszprunar, G. (1996). The molluscan rhogocyte (pore-cell, Blasenzelle, cellule nucale), and its significance for ideas on nephridial evolution. *Journal of Molluscan Studies, 62*, 185–211.

Healy, J. M. (1990). Spermatozoa and spermiogenesis of *Cornirostra*, *Valvata* and *Orbitestella* (Gastropoda, Heterobranchia) with a discussion on valvatoidean sperm morphology. *Journal of Molluscan Studies, 56*, 557–566.

Healy, J. M. (1993). Comparative sperm ultrastructure and spermiogenesis in basal heterobranch gastropods (Valvatoidea, Architectonicoidea, Rissoelloidea, Omalogyroidea, Pyramidelloidea). *Zoologica Scripta, 22*, 263–276.

Hedegaard, C. (1990). *Shell structure of the Recent Archaeogastropoda*. PhD thesis. Aarhus, Denmark: University of Aarhus.

Herbert, D. G. (1982). Fine structural observations on the juxtaganglionar organ of *Gibbula umbilicalis* (Da Costa). *Journal of Mollusan Studies, 48*, 226–228.

Heß, M., Beck, F., Gensler, H., Kano, Y., Kiel, S., & Haszprunar, G. (2008). Microanatomy, shell structure and molecular phylogeny of *Leptogyra*, *Xyleptogyra* and *Leptogyropsis* (Gastropoda: Neomphalida: Melanodrymiidae) from sunken wood. *Journal of Molluscan Studies, 74*, 383–401.

Høisaeter, T., & Johannessen, P. J. (2002). *Xylodiscula planata* sp. nov., a "lower" heterobranch gastropod from Norwegian waters. *Sarsia, 86*, 325–332.

Jamieson, B. G. M. (1987). A biological classification of sperm types, with special reference to annelids and molluscs, and an example of spermiocladistics. In H. Mohri (Ed.), *New horizons in sperm cell research* (pp. 311–332). Tokyo: Japan Scientific Society Press.

Johansson, J. (1956). Garnault's duct and its significance for the phylogeny of the genital system of *Valvata*. *Zoologiska Bidrag från Uppsala, 30*, 457–464. pls. 1–2.

Jörger, K. M., Stöger, I., Kano, Y., Fukuda, H., Knebelsberger, T., & Schrödl, M. (2010). On the origin of Acochlidia and other enigmatic euthyneuran gastropods and implications for the systematics of Heterobranchia. *BMC Evolutionary Biology, 10*(323), 1–20.

Kruglow, N. D., & Frolenkova, O. A. (1981). Structure of egg-clutches in molluscs of the family Valvatidae (Pectinibranchia, Ectobranchia). [In Russian, with English abstract.] *Vestnik Leningradskogo Gosudarstvennogo Universiteta Biologichesky, 1981*(1), 52–58.

Kunze, T., & Haszprunar, G. (2008). What are skeneimorph gastropods? – How 3D based anatomy can help to shed some light on the polyphyletic assemblage called Skeneidae. *The Malacologist, 52*, 6–7.

Lindholm, W. A. (1927). *Valvata naticina* Menke und ihr Formenkreis. *Archiv für Molluskenkunde, 59*, 20–33.

Luchtel, D. L., Martin, A. W., Deyrup-Olsen, I., & Boer, H. H. (1997). Gastropoda: Pulmonata. In F. W. Harrison & A. J. Kohn (Eds.), *Microscopic anatomy of invertebrates, vol. 6B: Mollusca II* (pp. 459–718). New York: Wiley-Liss.

Marshall, B. A. (1988). Skeneidae, Vitrinellidae and Orbitestellidae (Mollusca, Gastropoda) associated with biogenic substrata from bathyal depths off New Zealand and New South Wales. *Journal of Natural History, 22*, 969–1004.

Marshall, D. J., & Hodgson, A. N. (1990). Structure of the cephalic tentacles of some species of prosobranch limpets (Patellidae and Fissurellidae). *Journal of Molluscan Studies, 56*, 415–424.

Martoja, M. (1965a). Existence d'un organe juxta-ganglionaire chez *Aplysia punctata* Cuv. (Gastéropode Opisthobranche). *Comptes Rendus de l'Academie des Sciences, Paris, 260*, 4615–4617.

Martoja, M. (1965b). Données relatives à l'organe juxta-ganglionaire des Prosobranches Diotocardes. *Comptes Rendus de l'Academie des Sciences, Paris, 261*, 3195–3196.

McArthur, A. G., & Harasewych, M. G. (2003). Molecular systematics of the major lineages of the Gastropoda. In C. Lydeard & D. R. Lindberg (Eds.), *Molecular systematics and phylogeography of mollusks* (pp. 140–160). Washington & London: Smithsonian Series on Evolutionary Biology. Smithsonian Books.

Monterosato, T. A. (1874). Recherches conchyliologiques, effectuées au Cap Santo Vito, en Sicilie. *Journal de Conchyliologie (Paris), 14*, 243–282.

Ponder, W. F. (1990a). The anatomy and relationships of the Orbitestellidae (Gastropoda: Heterobranchia). *Journal of Molluscan Studies, 56*, 515–532.

Ponder, W. F. (1990b). The anatomy and relationships of a marine valvatoidean (Gastropoda: Heterobranchia). *Journal of Molluscan Studies, 56*, 533–556.

Ponder, W. F. (1991a). Marine valvatoidean gastropods – implication for early heterobranch phylogeny. *Journal of Molluscan Studies, 57*, 21–32.

Ponder, W. F. (1991b). The anatomy of *Diala*, with an assessment of its taxonomic position (Mollusca: Cerithioidea). In F. E. Wells, D. I. Walker, H. Kirkman, & R. Lethbridge (Eds.), *The marine flora and fauna of Albany, Western Australia, vol. 2* (pp. 500–519). Perth: Western Australian Museum.

Ponder, W. F., & Lindberg, D. R. (1997). Towards a phylogeny of gastropod molluscs: an analysis using morphological characters. *Zoological Journal of the Linnean Society, 119*, 83–265.

Rath, E. (1986). *Beiträge zur Anatomie und Ontogenie der Valvatidae (Mollusca: Gastropoda)*. Unpublished dissertation. Vienna, Austria: Institut für Zoologie der Universität Wien.

Rath, E. (1988). Organization and systematic position of the Valvatidae. *Malacological Review, Supplement, 4*, 194–204.

Richardson, K. C., Jarett, L., & Finke, E. H. (1960). Embedding in epoxy resins for ultrathin sectioning in electron microscopy. *Stain Technology, 35*, 313–323.

Robertson, R. (1985). Four characters and the higher category systematics of gastropods. *American Malacological Bulletin, Special Edition, 1*, 1–22.

Robertson, R. (1993). Snail handedness. The coiling directions of gastropods. *National Geographic Research and Exploration, 9*, 104–119.

Romeis, B. (1989). *Mikroskopische Technik, 17th edition* [Böck, P. (Ed.)]. Munich, etc.: Urban & Schwarzenberg.

Rubio, F., Rolan, E., & Fernandes, F. (1992). Nueva especie de *Hyalogyra* (Archaeogastropoda: Skeneidae) procedente de la costa occidental Africana. *Bollettino di Malacologico, 28*, 145–148.

Ruthensteiner, B. (2008). Soft part 3D visualization by serial sectioning and computer reconstruction. In D. Geiger, & B. Ruthensteiner (Eds.), *Micromolluscs: methodological challenges – exciting results*. *Zoosymposia, 1*, 63–100.

Ruthensteiner, B., & Heß, M. (2008). Embedding 3D models of biological specimens in PDF publications. *Microscopy Research and Technique, 71*, 778–786.

Sahling, H., Rickert, D., Lee, R. W., Linke, P., & Suess, E. (2002). Macrofaunal community structure and sulfide flux at gas hydrate deposits from the Cascadia convergent margin, NE Pacific. *Marine Ecology Progress Series, 231*, 121–138.

Salvini-Plawen, L., & Haszprunar, G. (1987). The Vetigastropoda and the systematics of streptoneurous Gastropoda (Mollusca). *Journal of Zoology (London), 211*, 747–770.

Sasaki, T. (1998). Comparative anatomy and phylogeny of the recent Archaeogastropoda (Mollusca: Gastropoda). *University and Museum of Tokyo Bulletin, 38*, 1–224.

Simone, L. R. L. (1995). *Rissoella ornata*, a new species of Rissoellidae (Mollusca: Gastropoda: Rissoelloidea) from the southeastern coast of Brazil. *Proceedings of the Biological Society of Washington, 108*, 560–567.

Sitnikova, T. Y. (1984). Some aspects of the structure and functioning of the reproductive system of the family Valvatidae (Gastropoda, Pectinibranchia). [In Russian, with English abstract]. *Vestnik Leningradskogo Gosudarstvennogo Universiteta Biologichesky, 1984(2)*, 121–123.

Sminia, T., & Boer, H. H. (1973). Haemocyanin production in pore cells of the freshwater snail *Lymnaea stagnalis*. *Zeitschrift für Zellforschung, 145*, 443–445.

Sminia, T., De With, N. D., Bos, J. L., Van Nieuwmegen, M. E., Witter, M. P., & Wondergem, J. (1976). Structure and function of the calcium cells of the freshwater pulmonate snail *Lymnaea stagnalis*. *Netherlands Journal of Zoology, 27*, 195–208. pls. 1–3.

Speimann, E., Heß, M., & Haszprunar, G. (2007). 3D-anatomy of the rhipidoglossate heterobranchs *Hyalogyrina depressa* Hasegawa, 1997 and *Xenoskenea pellucida* (Monterosato, 1874) (Gastropoda, Ectobranchia). *Abstracts of the World Congress of Malacology, Antwerp, July, 2007*, 212–213.

Spurr, A. R. (1969). A low-viscosity epoxy resin embedding medium for electron microscopy. *Journal of Ultrastructural Research, 26*, 31–43.

Starmühlner, F. (1952). Zur Anatomie, Histologie und Biologie einheimischer Prosobranchier. *Österreichische Zoologische Zeitschrift, 3*, 546–590.

Switzer-Dunlap, M. F. (1987). Ultrastructure of the juxtaganglionar organ, a putative endocrine gland associated with the cerebral ganglion of *Aplysia juliana*. *International Journal of Invertebrate Reproduction and Development, 11*, 295–304.

Van den Biggelaar, J. A. M., & Haszprunar, G. (1996). Cleavage patterns in the Gastropoda: an evolutionary approach. *Evolution, 50*, 1520–1540.

Wägele, H., Klussmann-Kolb, A., Vonnemann, V., & Medina, M. (2008). Heterobranchia I. The Opisthobranchia. In W. F. Ponder & D. R. Lindberg (Eds.), *Phylogeny and evolution of the Mollusca* (pp. 383–406). Berkeley: University of California Press.

Warén, A. (1992). New and little known "skeneimorph" gastropods from the Mediterranean Sea and the adjacent Atlantic Ocean. *Bollettino di Malacologico (Milano), 27*, 149–248.

Warén, A., & Bouchet, P. (1993). New records, species, genera, and a new family of gastropods from hydrothermal vents and hydrocarbon seeps. *Zoologica Scripta, 22*, 1–90.

Warén, A., & Bouchet, P. (2001). Gastropoda and Monoplacophora from hydrothermal vents and seeps; new taxa and records. *Zoologica Scripta, 44*, 116–231.

Warén, A., & Bouchet, P. (2009). New gastropods from deep-sea hydrocarbon seeps off West Africa. *Deep-Sea Research II, 56*, 2326–2349.

Warén, A., Gofas, S., & Schander, C. (1993). Systematic position of three European heterobranch gastropods. *Véliger, 36*, 1–15.

Warén, A., Carozza, F., & Rocchini, R. (1997). Description of two new species of Hyalogyrinidae (Gastropoda, Heterobranchia) from the Mediterranean. *Bollettino Malacologico, 32*, 57–66.

Wise, J. B. (1998). Morphology and systematic position of *Rissoella caribaea* Rehder, 1943 (Gastropoda: Heterobranchia: Rissoellidae). *Nautilus, 111*, 13–21.

Yonge, C. M. (1947). The pallial organs in the aspidobranch gastropods and their evolution throughout the Mollusca. *Philosophical Transactions of the Royal Society of London/B, 232*, 443–518. 1 pl.